NAVAL POSTGRADUATE SCHOOL
Monterey, California

THESIS

EXPERIMENTAL INVESTIGATION OF VORTEX SHEDDING IN HIGH REYNOLDS NUMBER FLOW OVER COMPRESSOR BLADES IN CASCADE

by

Choon Peng, Lim

March 2003

Thesis Advisor:	Garth V. Hobson
Second Reader:	Raymond P. Shreeve

THIS PAGE INTENTIONALLY LEFT BLANK

REPORT DOCUMENTATION PAGE			Form Approved OMB No. 0704-0188
Public reporting burden for this collection of information is estimated to average 1 hour per response, including the time for reviewing instruction, searching existing data sources, gathering and maintaining the data needed, and completing and reviewing the collection of information. Send comments regarding this burden estimate or any other aspect of this collection of information, including suggestions for reducing this burden, to Washington headquarters Services, Directorate for Information Operations and Reports, 1215 Jefferson Davis Highway, Suite 1204, Arlington, VA 22202-4302, and to the Office of Management and Budget, Paperwork Reduction Project (0704-0188) Washington DC 20503.			
1. AGENCY USE ONLY *(Leave blank)*	**2. REPORT DATE** March 2003	**3. REPORT TYPE AND DATES COVERED** Master's Thesis	
4. TITLE AND SUBTITLE: Experimental Investigation of Vortex Shedding in High Reynolds Number Flow Over Compressor Blades in Cascade			**5. FUNDING NUMBERS**
6. AUTHOR(S) Choon Peng, Lim			
7. PERFORMING ORGANIZATION NAME(S) AND ADDRESS(ES) Naval Postgraduate School Monterey, CA 93943-5000			**8. PERFORMING ORGANIZATION REPORT NUMBER**
9. SPONSORING / MONITORING AGENCY NAME(S) AND ADDRESS(ES)			**10. SPONSORING / MONITORING AGENCY REPORT NUMBER**
11. SUPPLEMENTARY NOTES The views expressed in this thesis are those of the author and do not reflect the official policy or position of the Department of Defense or the U.S. Government.			
12a. DISTRIBUTION / AVAILABILITY STATEMENT Approved for public access; distribution is unlimited			**12b. DISTRIBUTION CODE**

13. ABSTRACT ***(maximum 200 words)***

An investigation of vortex shedding downstream of a cascade of compressor stator blades, at off-design inlet-flow angles of 35, 33 and 31 degrees and Reynolds numbers, based on chord length, of 625,000, 750,000 and 800,000 is reported.

The objective of the study was to characterize the flow and vortex shedding through blade surface pressure measurements and hot-wire anemometry. Vortex shedding was determined to be a leading edge phenomenon as periodic shedding was only detected on the pressure side of the wake. The relationship between vortex shedding frequency and Reynolds number was nearly linear. The vortex shedding frequency at three incidence angles was observed to be quite similar at lower Reynolds number (i.e. 450,000 and below) but developed into a larger scatter at higher Reynolds number. Similarly, the Strouhal numbers were observed to be fairly consistent (0.22 to 0.24) at low Reynolds number and more scattered (0.18 to 0.25) with increasing Reynolds number. The result obtained was comparable to the experimental results obtained by Roshko[Ref. 14], for vortex shedding behind a circular cylinder.

14. SUBJECT TERMS Controlled-diffusion, Compressor, Stator, Cascade, Turbomachinery, Hot-wire anemometry, Laser-Doppler velocimetry, Vortex shedding			**15. NUMBER OF PAGES** 97
			16. PRICE CODE
17. SECURITY CLASSIFICATION OF REPORT Unclassified	**18. SECURITY CLASSIFICATION OF THIS PAGE** Unclassified	**19. SECURITY CLASSIFICATION OF ABSTRACT** Unclassified	**20. LIMITATION OF ABSTRACT** UL

NSN 7540-01-280-5500 Standard Form 298 (Rev. 2-89)
Prescribed by ANSI Std. 239-18

THIS PAGE INTENTIONALLY LEFT BLANK

Approved for public release; distribution is unlimited

EXPERIMENTAL INVESTIGATION OF VORTEX SHEDDING IN HIGH REYNOLDS NUMBER FLOW OVER COMPRESSOR BLADES IN CASCADE

Choon Peng, Lim
Major, Republic of Singapore Air Force
B.E., Mechanical, Nanyang Technological University, 1996

Submitted in partial fulfillment of the
requirements for the degree of

MASTER OF SCIENCE IN AERONAUTICAL ENGINEERING

from the

NAVAL POSTGRADUATE SCHOOL
March 2003

Author: Choon Peng, Lim

Approved by: Garth V. Hobson
Thesis Advisor

Raymond P. Shreeve
Second Reader

Max F. Platzer
Chairman, Department of Aeronautics and Astronautics

THIS PAGE INTENTIONALLY LEFT BLANK

ABSTRACT

An investigation of vortex shedding downstream of a cascade of compressor stator blades, at off-design inlet-flow angles of 35, 33 and 31 degrees and Reynolds numbers, based on chord length, of 625,000, 750,000 and 800,000 is reported.

The objective of the study was to characterize the flow and vortex shedding through blade surface pressure measurements and hot-wire anemometry. Vortex shedding was determined to be a leading edge phenomenon as periodic shedding was only detected on the pressure side of the wake. The relationship between vortex shedding frequency and Reynolds number was nearly linear. The vortex shedding frequency at three incidence angles was observed to be quite similar at lower Reynolds number (i.e. 450,000 and below) but developed into a larger scatter at higher Reynolds number. Similarly, the Strouhal numbers were observed to be fairly consistent (0.22 to 0.24) at low Reynolds number and more scattered (0.18 to 0.25) with increasing Reynolds number. The result obtained was comparable to the experimental results obtained by Roshko [Ref. 14], for vortex shedding behind a circular cylinder.

THIS PAGE INTENTIONALLY LEFT BLANK

TABLE OF CONTENTS

LIST OF FIGURES

THIS PAGE INTENTIONALLY LEFT BLANK

ACKNOWLEDGMENTS

I am thankful to my advisor, Professor Garth Hobson, for this guidance, enthusiasm and patience towards the project. I would also like to thank Rick Still and John Gibson for their prompt technical support and friendship. I would also like to acknowledge all the wonderful guys in the Propulsion Laboratory, including Professor Shreeve and Anthony Gannon for their friendship and encouragement.

Finally, I am grateful to my wife, Chiew Ping, for her love, understanding, patience and steadfast support, despite all the difficulties along the way.

THIS PAGE INTENTIONALLY LEFT BLANK

I. INTRODUCTION

A. BACKGROUND

The continual demand for smaller and more powerful engines for today's civil and military aircraft has led to increased requirements for blade loading, improved performance at the design point and perhaps most importantly, the ability to operate at off-design conditions without adverse effects such as compressor stall. These demands have led to the development of Controlled-Diffusion (CD) blading. Controlled-Diffusion blading allows blades to be specifically designed to produce a desired pressure distribution, while simultaneously avoiding boundary-layer separation on the suction side of the blade. This leads to higher blade loading and more turning for each blade row. The increased loading results in a higher pressure ratio with the same number of blades or fewer blade rows for a desired pressure. Both options will result in significant size and weight reduction for a desired thrust level.

Controlled-Diffusion blading design also results in profiles that have relatively blunt leading and trailing edges, from which vortex shedding might occur at various off-design conditions. Vortex shedding in turbomachinery can result in flow unsteadiness in excess of 20 KHz, which is higher than either blade passing frequencies or background turbulence. These unsteady flow phenomena could lead to high cycle fatigue problems within engine components. The first step towards resolving these high cycle fatigue concerns is to understand all the unsteady flow processes within blade rows and the effect these will have on blade loading levels.

The CD compressor blades investigated in the current study were designed by Thomas F. Gelder of NASA Lewis Research Center, for a design inlet-flow angle of 36 degrees [Ref. 1]. The compressor stator profiles were Stator 67B blades, which together with Rotor 67, comprised Compressor Stage 67B. The Stator 67B blades were second-generation CD blades, which were designed as an improvement over Stator 67A, a first-generation CD blade designed by Nelson Sanger [Ref. 2].

The present study was an investigation of flow through Compressor Stage 67B CD compressor blades in the Naval Postgraduate School (NPS) low-speed cascade wind tunnel (LSCWT). Hanson [Ref. 3] examined the flow through the mid-span section at a near-design inlet-flow angle of 36.3 degrees, using Laser-Doppler Velocimetry (LDV) and pressure probe measurements. Schnorenberg [Ref. 4] studied the off-design flow characteristics at an angle of 38 degrees, using LDV measurements, flow visualization, and blade surface pressure measurements to investigate the effect of Reynolds number on a separation region detected near mid-chord. Grove [Ref. 5] characterized the flow patterns at an inlet-flow angle of 39.5 degrees, with flow visualization, rake probe surveys, blade surface pressure measurements and LDV measurements. Nicholls [Ref. 6] characterized and compared the flow patterns over and around the blades after the replacement of the wind tunnel motor. The inlet-flow angle was found to have increased from 39.5 to 40 degrees with no reconfiguration of the tunnel. Carlson [Ref. 7] characterized the three-dimensional flow behavior in the end-wall region of the cascade using five-hole pressure probe and two-component LDV measurements. CFD studies were also initiated to compare blade surface pressure distributions at various inlet-flow angles and inlet boundary layer thicknesses. Caruso [Ref. 8] conducted an off-design (38 degrees) investigation of the three-dimensional flow field ahead of and behind the blades using three-component LDV, and detailed the complex flow field including the corner vortex system. More recently, Brown [Ref. 9], conducted an investigation of the vortex shedding phenomenon at three Reynolds numbers and three inlet-flow angles, using various complementary methods, including hot-wire anemometry, five-hole probe wake surveys and LDV.

B. PURPOSE

The objective of the present study was to locate, identify and characterize vortex shedding over the blades at three different off-design inlet-flow angles of 31, 33 and 35 degrees, and three Reynolds numbers based on chord length, at 625,000, 750,000 and 800,000. Various methods were used including surface pressure measurements and hot-wire anemometry. Two-component LDV inlet surveys were performed to ensure correct inlet-flow angle settings.

THIS PAGE INTENTIONALLY LEFT BLANK

II. TEST FACILITY AND INSTRUMENTATION

A. LOW-SPEED CASCADE WIND TUNNEL

The present study was conducted in the Low-Speed Cascade Wind Tunnel (LSCWT) located at the Naval Postgraduate School's Turbopropulsion Laboratory. The wind tunnel is powered by a 550-hp electric motor driving a turbo-vane blower. It is capable of producing a sustained freestream Mach number of 0.4 in the test section. Figure II.1 shows a schematic of the cascade in the Low Speed Turbomachinery Building (Bldg. 213) with the associated plenum chamber, drive system, and inlet and exhaust ducting. All aspects of the tunnel remain as previously documented by Nicholls [Ref. 6].

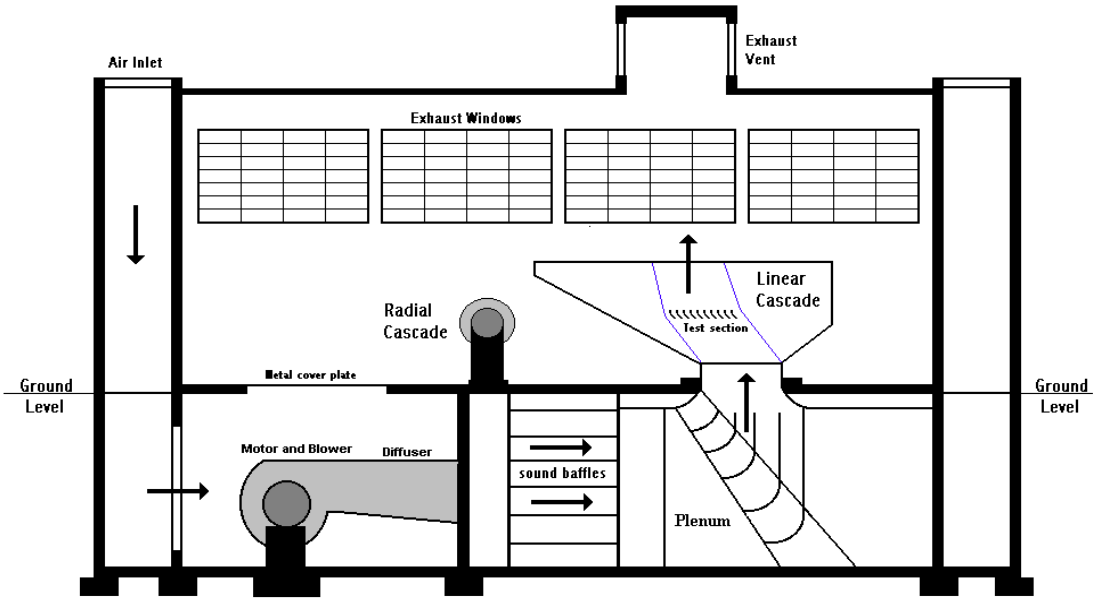

Figure II.1 NPS cascade wind tunnel facility

B. TEST SECTION

The test section of the LSCWT contained ten Controlled-Diffusion (CD) stator blades. Hansen [Ref. 3] documented the installation procedures of the blades in the test section. A detailed layout of the test section is shown in Figure II.2. Schnorenberg [Ref. 4] documented the procedure used to adjust the inlet-flow angle.

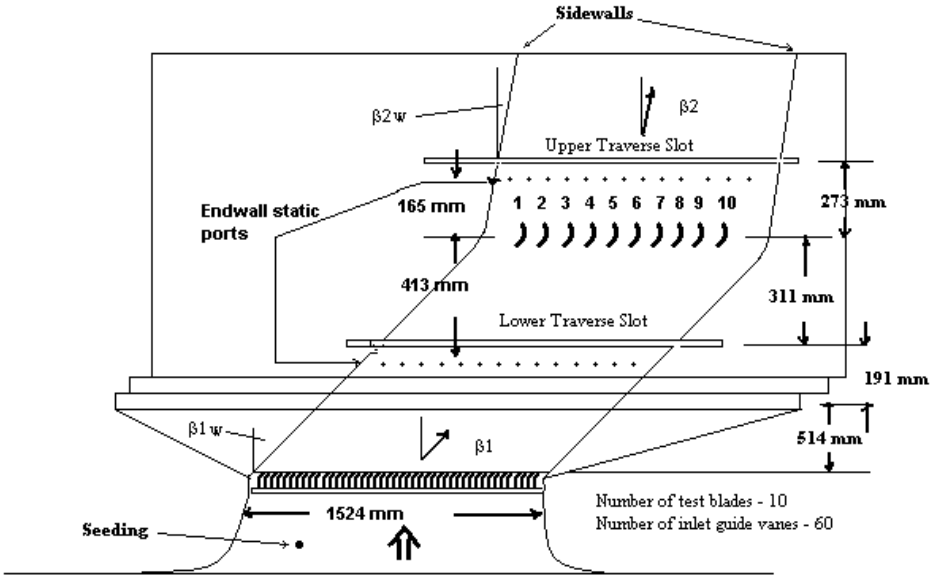

Figure II.2 Test section schematic

The blades were scaled from the mid-span section of the Stator 67B [Ref. 1]. Hanson [Ref. 3] documented the coordinates used to machine the blades. Each blade was 254 mm in span, 127.25 mm in chord and installed at a blade spacing of 152.4 mm.

The blade profile is shown in Figure II.3.

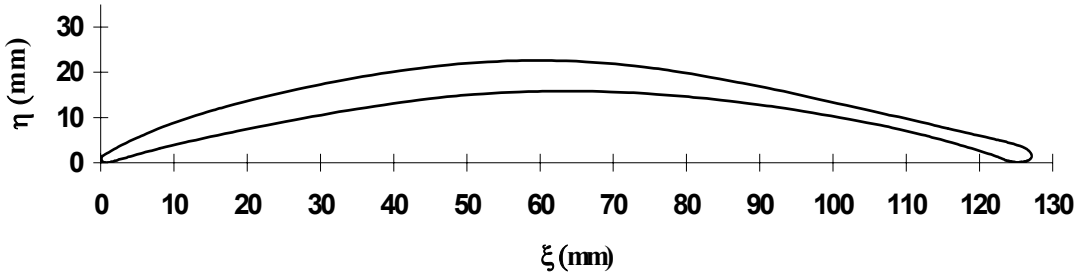

Figure II.3 Blade profile

Blades 2 and 8 (Figure II.4) were partially instrumented with eight pressure ports, and blade 6 was fully instrumented with 42 pressure ports around the blade profile at mid-span.

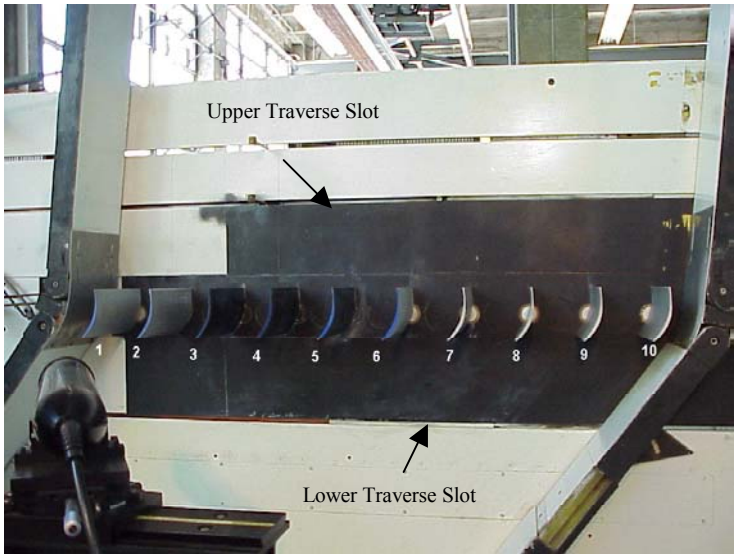

Figure II.4 CD blades mounted in LSCWT

Five-hole probe measurements were conducted in the wake across blades 3 and 4. The probe was positioned in the upper traverse slot, which was approximately 191 mm downstream of the blade trailing edge. Hot-wire measurements were conducted across blade 3, using the upper traverse slot, but with the probe positioned approximately 3 mm (~ 1.5% chord) downstream of the blade trailing edge. LDV measurements were conducted across the inlet of blades 3 and 4, which were anodized black to reduce laser light backscatter. Inlet-flow angle LDV measurements were conducted at 38.2 mm (~ 30% chord) upstream of the leading edges.

C. INSTRUMENTATION AND DATA ACQUISITION

1. Pressure Surveys

Surface pressure measurements were taken from the fully instrumented blade 6 and recorded as described by Grove [Ref. 5], to determine the pressure distribution over the surface of the blade and to locate areas of flow separation. All pressures from the instrumented blades were recorded using a 48-channel rotary pressure scanner as described by Carlson [Ref. 7]. Scanivalve ports and channel assignments are given in Appendix A. All pressure data were acquired using the HP75000 Series B VXI-Bus Mainframe controlled by HP-VEE software running on a PC. Grossman [Ref. 12]

documented the operation of the data acquisition system. Nicholls [Ref. 6] documented the HP-VEE program that was used to control the Scanivalve rotary pressure scanner.

2. Hot-Wire Anemometry

Hot-wire anemometry measurements were conducted to characterize, in detail, the flow in the wake of the blades, and to resolve the frequency and magnitude of the unsteady flow downstream of the blades. Measurements were taken with 20 micron TSI Model 1210-20 hot-film probes (Figure II.5) with individual serial numbers 014057 (for inlet-flow angle 31 and 35 degrees) and 121014 (for inlet-flow angle 33 degrees). A custom-built probe holder provided support for the probes. The probe holder stabilized the hot-film probes and allowed the probes to translate in the upper traverse slot in the LSCWT.

Figure II.5 Probe holder with hot-film probe installed

Hot-wire data were acquired and reduced using an IFA 100 Intelligent Flow Analyzer, and TSI ThermalPro software version 4.50.03, running on a PC. Figure II.6 shows the IFA 100 data acquisition system. Operational procedures can be found in Appendix B.

Figure II.6 IFA 100 data acquisition system

3. LDV Instrumentation and Data Acquisition

LDV measurements were obtained using a TSI two-component fiber-optic system. The system included a five-watt Lexel Model 95 argon-ion laser, directed into a TSI Model 9201 Colorburst multicolor beam separator, transmitted by fiber-optic cables to two 83 mm probes. The reflected signals were collected by the probes and fed back to a TSI Model 9230 Colorlink, via a return fiber-optic cable. Caruso [Ref. 8] documented the description of the laser, optics system, data acquisition system, and laser flow seeding system and traverse mechanism. All LDV data were acquired and reduced using TSI Find For Windows software, version 1.4. Figure II.7 shows the fiber optic probes, traverse mechanism and data acquisition system of the LDV setup. Figure II.8 shows the inlet-flow angle survey being performed using LDV. Operational procedure for the inlet flow angle survey is given in Appendix C.

Figure II.7 LDV optics, traverse and data acquisition system

Figure II.8 Inlet-flow angle survey using LDV

III. EXPERIMENTAL PROCEDURE

A. REYNOLDS NUMBER AND INLET-FLOW ANGLE VARIATION

To characterize the phenomenon of vortex shedding across the blades, data were collected at three Reynolds Number (625,000, 750,000 and 800,000) and three inlet- flow angles (31, 33 and 35 degrees).

The reference velocity (V_{ref}) was determined by measuring the delta pressure obtained from the pitot-static tube located upstream of the test section. The software that converted the pressure differential into velocity resided in the ThermoPro software used for hot-wire anemometry (i.e. "dP and Vel Calc" function). The Reynolds number was determined from the equation, $Re = \rho * V_{ref} * l / \mu$. The reference length ($l$) was the blade chord (i.e. 0.127 meter). The air density and viscosity used were the standard sea level conditions (i.e. 1.225 kg/m^3 and 1.7894E-05 kg/m-sec).

The tunnel was run at plenum pressures of about 317.5 mm (12.5 inches), 469.9 mm (18.5 inches) and 520.7 mm (20.5 inches) of water, corresponding to Reynolds numbers of 625,000, 750,000 and 800,000 respectively. These Reynolds numbers corresponded to freestream Mach numbers of 0.29, 0.34 and 0.37 respectively.

The cascade inlet walls were initially set at $\beta_{1W} = 31°$ (-5°incidence) giving $\beta_1 = 31.2°$ and the tailboards were set at β_{2W} (West) = 2.2° and β_{2W} (East) = 2.1°. Subsequent reconfigurations of the tunnel positioned the inlet walls at $\beta_{1W} = 35°$ (-1° incidence) giving $\beta_1 = 35.2°$ with tailboard settings of 3.5° (West) and 3.8° (East); and finally, $\beta_{1W} = 33°$ (-3° incidence) giving $\beta_1 = 33.2°$, with tailboards set at 3.8° (West) and 1.8° (East).

B. PRESSURE MEASUREMENTS

The cascade tunnel was allowed to reach an equilibrium plenum temperature prior to all surveys, approximately 0.5 hour. Blade surface pressure measurements were taken from the fully instrumented blade number 6, using the HP Automated Data Acquisition System and Scanivalve #1. Data acquisition was performed using a HP-VEE program with filename "Blade_Cp". Inlet total and static pressures were recorded to non-dimensionalize the blade surface pressure measurements as a coefficient of pressure; i.e., $Cp = (plocal - p\infty) / (pt\infty - p\infty)$. The pitot and static pressures were measured using Scanivalve #2 and an HP-VEE program with filename "Fivehole". The data were exported to a spreadsheet developed by Brown [Ref. 9], for processing and analysis. A complete description of the calibration and operational procedures is presented in Appendix C.

C. HOT-WIRE ANEMOMETRY

1. IFA 100 and Hot-Wire Calibration

The cable resistance was measured on the IFA 100 with the shorting probe inserted in place of the hot-film probe. Then the hot-film probe resistance was measured by replacing the shorting probe with the hot-film probe. The operating resistance was set based on the recommended value stated on the probe data sheet. Then the bridge compensation was set and the no-flow voltage (Eo) was noted. The tunnel was started and set at 533.4 mm (21 inches) of water, plenum pressure. The cable compensation was adjusted, noting the voltage (Em) at high flow. From the high flow voltage, no-flow voltage, and probe resistance, span, offset and gain were calculated and set on the IFA 100. The calculation and parameter setting were performed using the ThermoPro software.

The *in-situ* calibration run of the hot film consisted of recording plenum pressure, plenum temperature, pitot-static pressure and voltage data at each of the ten discrete plenum pressure settings between zero and 533.4 mm (21 inches) of water. During the

run, the hot-film probe was positioned 25 mm from the downstream pitot-static tube for velocity correlation. The calibration curves and King's Law coefficients were calculated by the ThermoPro software and saved in a calibration file. Descriptions of the calibration and operational procedures are presented in Appendix B.

2. Hot-Wire Wake Surveys

Data acquisition files were created with the appropriate calibration information and specific probe data. Data were taken by traversing the hot-film probe 76.2 mm across the blade passages (38.1 mm either side of the centerline of the trailing edge) downstream of blade 3. The probe was traversed at the minimum attainable increment of 1.27 mm, producing 60 discrete data points per survey. A survey was conducted for each Reynolds number (625,000, 750,000 and 800,000) at each inlet-flow angle (31, 33 and 35 degrees). At each point in the survey, 8000 samples were recorded at a rate of 40K samples per second. Atmospheric pressure and temperature, as well as plenum pressure and temperature were recorded for each run. Raw data were reduced using the ThermalPro software version 4.50.03. Data were normalized to a reference velocity calculated for the particular inlet-flow angle and Reynolds number. The mean velocity and turbulence intensity distribution across the wake were plotted for analysis.

3. Strouhal Number Survey

From the processed data files, the frequency power spectrum plots were analyzed for the presence of vortex shedding. A frequency spike on the power spectrum plot indicated the existence of vortex shedding from the trailing edge. Strouhal numbers were calculated as $St = \omega D/U_{mean}$, based on the leading edge diameter (D) of 4 mm and the freestream U_{mean} outside the wake. After determining the location of vortex shedding, a survey was conducted by increasing the tunnel Reynolds number. Data samples were taken at two locations on either side of the known location of vortex shedding. The frequency power spectrum for each sample of data from the five locations was analyzed for existence of vortex shedding. Once the existence of vortex shedding was confirmed, the Strouhal number was calculated for the corresponding Reynolds number.

D. LDV MEASUREMENTS

1. Inlet Guide Vane Adjustment

The tunnel was reconfigured twice to set nominal off-design inlet-flow angles of 31, 33 and 35 degrees. After each reconfiguration, prior to any data collection, LDV inlet surveys were conducted at Station 1, over one full passage (152.4 mm), to determine the mean flow angle downstream of the inlet guide vanes ($\beta 1$). Inlet guide vanes were adjusted until the mean flow-angle was within 0.2 degrees of the desired inlet-flow angle of the blades.

2. Particle Seeding

Vegetable oil was used as the seeding material for the present study. The seed particle generator used was a TSI Model 9306 6-jet atomizer modified as shown and described by Caruso [Ref. 8]. The four adjustable wands provided adequate seeding coverage for the survey area.

3. LDV Inlet Surveys

Two LDV inlet surveys were performed to check the inlet flow angle. They were performed at inlet-flow angles of 33 and 35 degrees. All surveys were conducted at midspan and at a plenum pressure of 304.8 mm (12 inches) of water. Inlet-flow surveys were conducted at Station 1, from the leading edge of blade 3 to the leading edge of blade 4 (152.4 mm), in 6.35 mm increments. Prior to each set of surveys, the laser beams were tuned using a Newport Model 815 digital power meter. Surveys were conducted at 0.75 watts of laser power. Five MHz of frequency shifting was used for data acquisition and all histograms used 1000 points. A complete description of the operational procedures is presented in Appendix D.

IV. RESULTS AND DISCUSSION

A. SURFACE PRESSURE MEASUREMENTS

The surface pressure measurements were taken from the fully instrumented blade 6. Measurements were taken at three different Reynolds numbers (i.e. 625,000, 750000 and 800,000) and at each inlet-flow angle (31°, 33° and 35°). The blade surface pressure measurements were non-dimensionalized using inlet total and static pressures. The surface pressure distributions are presented in terms of the coefficient of pressure (CP) plotted against fraction of the blade chord (x/c). Data were included for lower Reynolds numbers (i.e. 280,000, 380,000 and 640,000), which were obtained from the earlier work done by Brown [Ref. 9]. Corrections were made to the Reynolds numbers computed by Brown because he inferred the Reynolds number from the plenum pressure reading instead of determining the correct Reynolds number from the actual inlet velocity. The inlet velocity was obtained from the pitot-static tube inserted upstream.

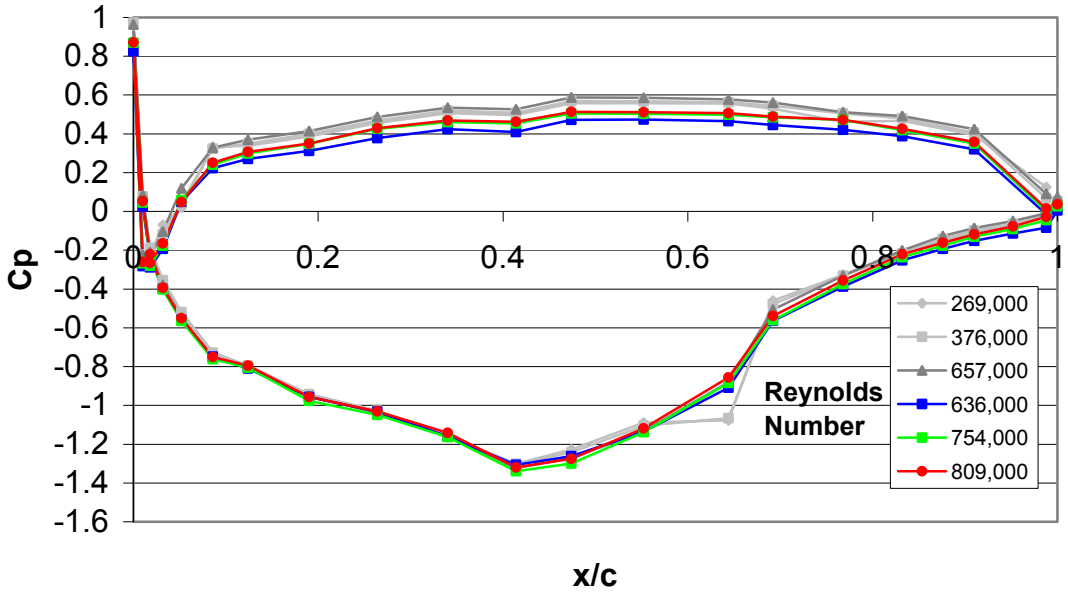

Figure VI.1 C_P versus X/C for inlet-flow angle of 35 degrees

The six surface pressure distributions for an inlet-flow angle of 35 degrees (-1° incidence) are shown in Figure VI.1. The suction side C_P is shown to decrease almost immediately at the leading edge to a value of -0.75. The acceleration of the flow continued to 0.41 x/c where the C_P reached its minimum value of -1.34. From 0.41, the suction side pressure distribution increased with no sign of separation until 0.55 x/c. Between 0.55 and 0.68 x/c, the adverse pressure gradient caused laminar flow separation on the blade surface at Reynolds number 376,000 and below. At higher Reynolds number, the boundary layer underwent transition ahead of the bubble, which energized the velocity profile at the blade surface, and partially suppressed the separation bubble. The observed behavior was similar to that measured at positive incidence by Schnorenberg [Ref. 4]. The C_P distribution over the pressure side after an initial spike was smooth and constant to the trailing edge, with no evidence of separation.

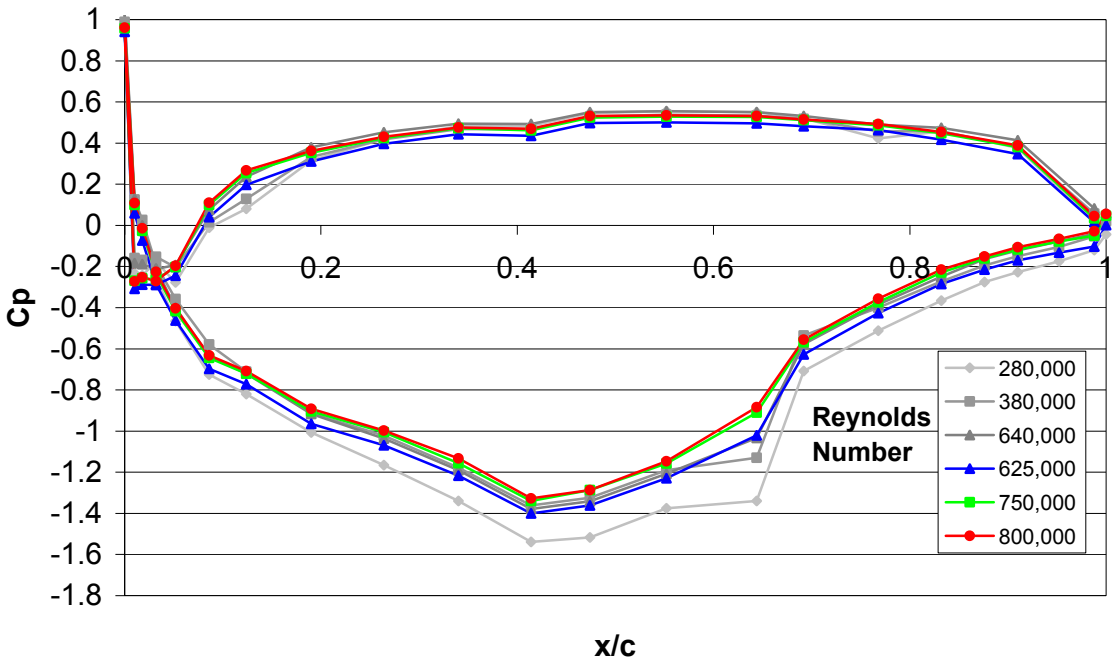

Figure VI.2 C_P versus X/C for inlet-flow angle of 33 degrees

The six surface pressure distributions for an inlet-flow angle of 33 degrees (-3° incidence) are shown in Figure VI.2. The suction side C_P is seen to decrease at the leading edge to a value of -0.68. The acceleration of the flow continued again to 0.41 x/c where the C_P reached its minimum value of -1.37. From 0.41, the suction side pressure

distribution increased with no sign of separation until 0.55 x/c. Between 0.55 and 0.68 x/c, an adverse pressure gradient existed causing laminar flow separation on the blade. At higher Reynolds number, the boundary layer underwent transition ahead of the bubble, which energized the velocity profile at the blade surface, and partially suppressed the separation bubble. The C_P distribution on the pressure side showed that the initial spike at x/c ≈ 0.01 had grown, in extent, giving rise to a pressure plateau between x/c = 0.01 and x/c = 0.05. This was indicative of an existence of a leading edge separation bubble on the pressure side.

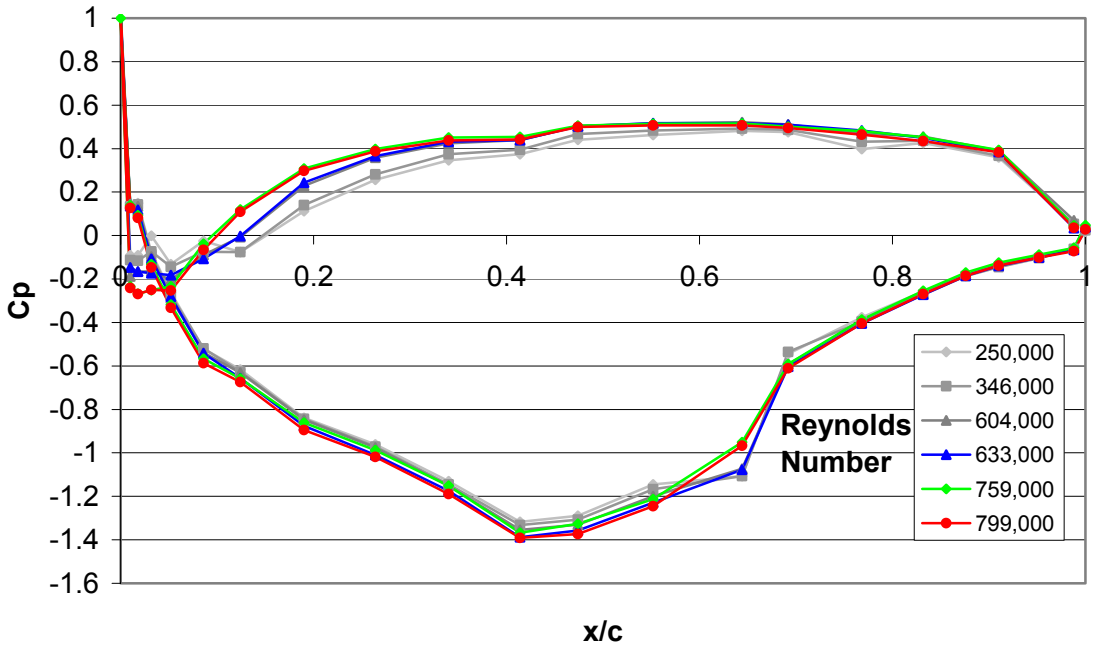

Figure VI.3 C_P versus X/C for inlet-flow angle of 31 degrees

The six surface pressure distributions for an inlet-flow angle of 31 degrees (-5° incidence) are shown in Figure VI.3. The suction side C_P decreased at the leading edge to a value of -0.58. Acceleration of the flow continued to 0.41 x/c where the C_P reached its minimum value of -1.35. From 0.41 x/c to 0.55 x/c the C_P increased linearly, showing no sign of separation. Between 0.55 and 0.68, an adverse pressure gradient existed, causing laminar flow separation on the blade. The C_P distribution on the pressure side showed that the initial spike at x/c ≈ 0.01 had grown even larger, and the pressure plateau

extended between x/c = 0.01 and x/c = 0.125; again indicative of a pressure side, leading edge separation bubble.

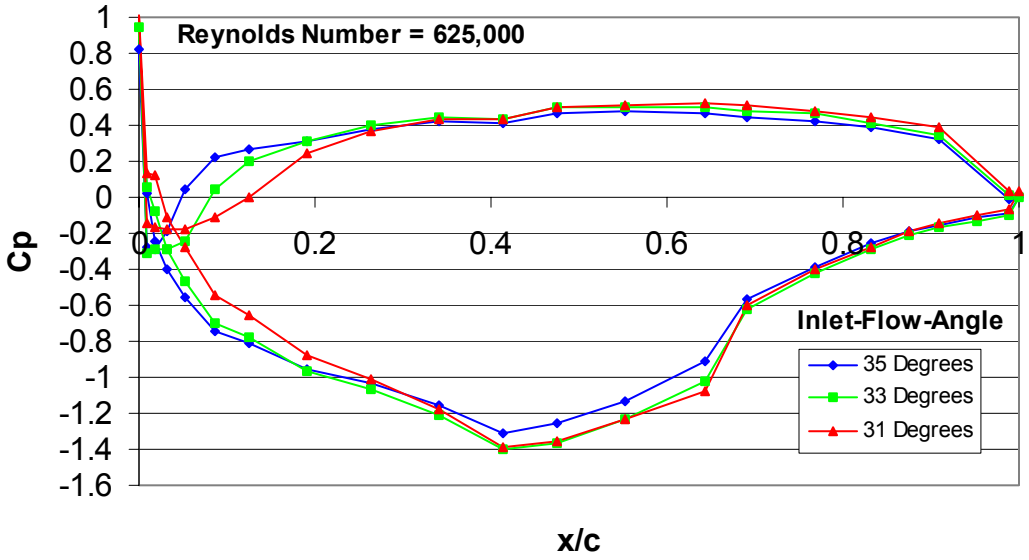

Figure VI.4 C_P versus X/C plot for three inlet-flow angles

By combining the pressure plots at different inlet-flow angle but at a common Reynolds number (i.e. 625,000), as shown in Figure VI.4, the following observations were noted:

a. There was no significant difference on the location and magnitude of the separation bubble on the suction side with change in incidence angles

b. The pressure plateau on the pressure side extended between x/c = 0.01 to x/c = 0.125 with corresponding decrease in incidence angles

c. The increases in pressure coefficient (C_P) were less gradual with corresponding decrease in incidence angles

As noted in Sanz and Platzer [Ref. 13], a strong adverse pressure gradient at the leading edge forced the laminar boundary layer to separate. The fluctuations in the separated shear layer caused rapid transition. The turbulent flow entrained more fluid and therefore caused the shear layer to bend toward the solid wall, which caused the flow

to re-attach as a turbulent boundary layer. As observed from Figure VI.4, the rise of the pressure coefficient at the leading edge at lower incidence angle (i.e. inlet-flow angle 31 degrees) was less gradual as compared to those near the design incidence angle (i.e. inlet-flow angle 35 degrees). Therefore, it was inferred that the size of the leading edge separation bubble and the laminar to turbulent transition region were significantly larger for flows at decreasing off-design incidence angles.

B. WAKE FLOW SURVEYS

The characterization of the trailing edge wakes were achieved through the use of hot-wire anemometry. The probe was located at 3.2 mm (1/8 inch) downstream of the trailing edge of blade 3. Surveys were taken at three Reynolds number (625,000, 750,000 and 800,000) and three inlet-flow angles (31, 33 and 35 degrees). Mean velocity profile and turbulence intensity plots were developed and analyzed. The mean velocity profile plots were illustrated by the non-dimensionalized velocity (U_{mean} / V_{ref}) on the y-axis and the probe location divided by span (i.e. 152.4 mm or 6 inches) on the x-axis. The reference velocity (V_{ref}) was computed from the pitot-static pressure measured in the inlet flow. The turbulence intensity plots were illustrated by the measured turbulence intensity (%) on the y-axis with the probe location divided by span on the x-axis.

The wake mean flow velocity profile at inlet-flow angle of 35 degrees (-1 degree incidence) is shown in Figure VI.5. The freestream velocity profile showed that a maximum was reached on either side of the wake, and a minimum at the center of the wake passage. The velocity ratio (U_{mean} / V_{ref}) was lower on the pressure side as compared to the suction side. This wake characteristic was due to the blade contour. Flow along the suction side of the blade accelerated more than on the pressure side. The pressure side entry into the wake was visibly steeper than the suction side, but otherwise, the wake was relatively symmetric and well defined. It was also observed that the width of the wake deficit increased along with an increase in Reynolds number.

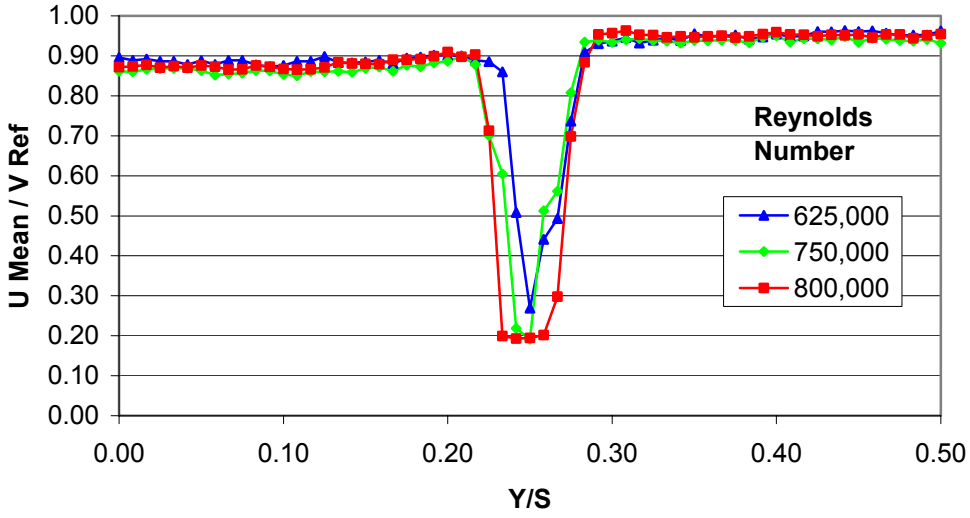

Figure VI.5 Wake mean flow velocity profiles at inlet-flow angle of 35 degrees

The wake mean flow velocity profile at inlet-flow angle of 33 and 31 degrees (-3 and –5 degrees incidence) are shown in Figure VI.6 and Figure VI.7. The wake mean flow velocity profile at inlet-flow angle of 33 degrees and 31 degrees were similar to those at 35 degrees inlet-flow angle. The pressure side entry into the wake was visibly steeper than the suction side, but otherwise, the wake was relatively symmetric and well defined. It was also observed that the width of the wake deficit increased along with an increase in Reynolds number.

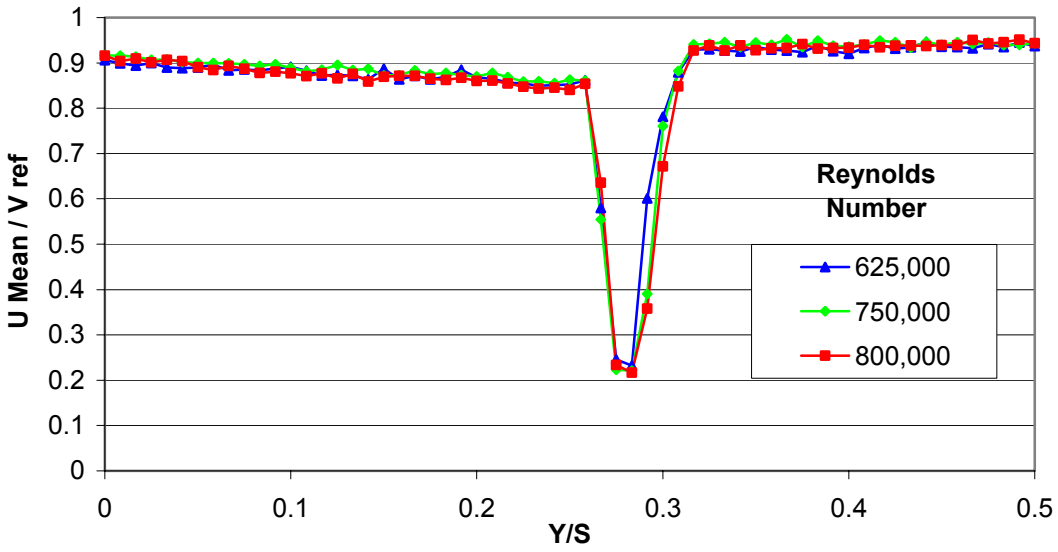

Figure VI.6 Wake mean flow velocity profile at inlet-flow angle of 33 degrees

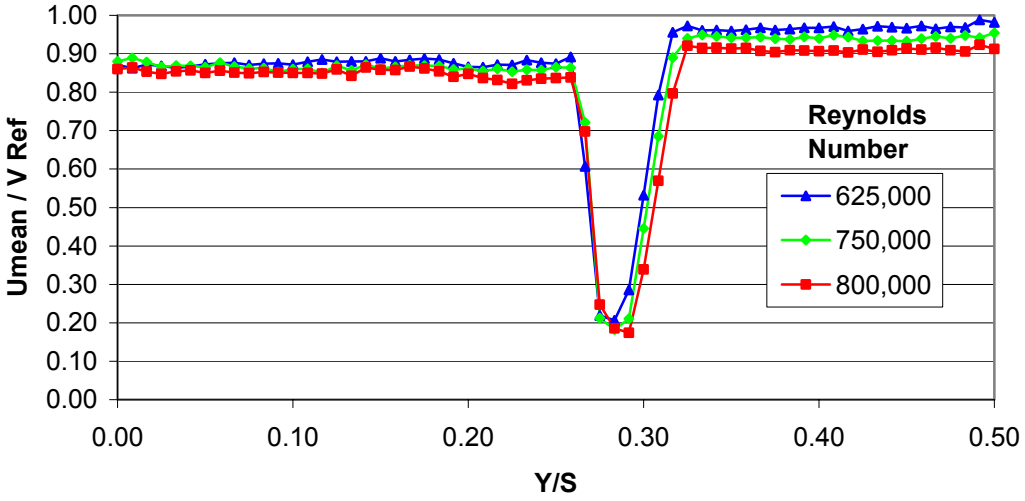

Figure VI.7 Wake mean flow velocity profile at inlet-flow angle of 31 degrees

By combining the mean velocity profile plots at different inlet-flow angles but at a common Reynolds number (i.e. 625,000), as shown in Figure VI.8, it was observed that the gradient of the velocity drop at the pressure side was more severe and the size of the

wake deficit was larger for 31 degrees (-5 degrees incidence) inlet-flow angle as compared to 35 degrees (-1 degree incidence).

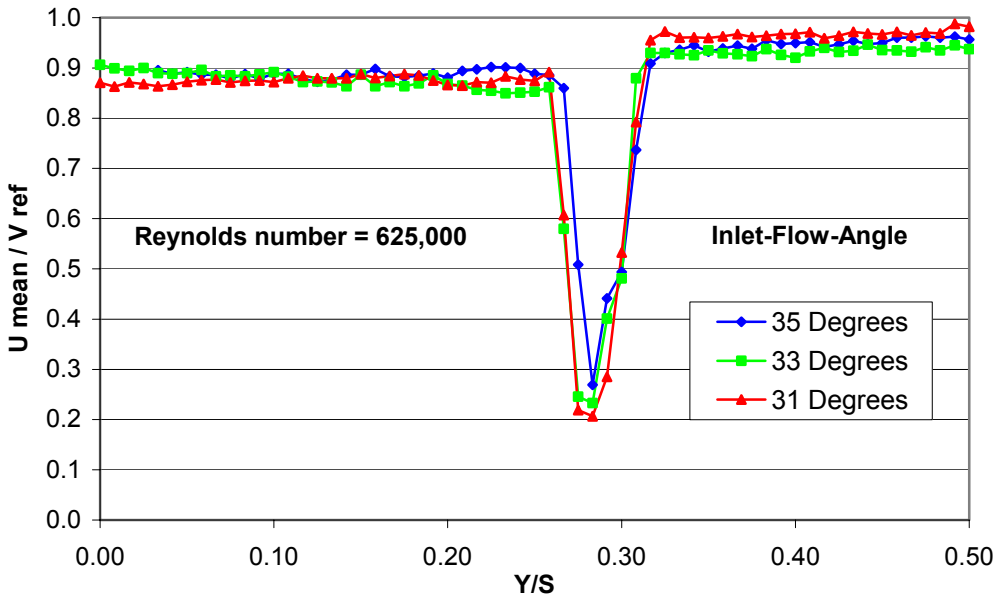

Figure VI.8 Wake mean flow velocity profile at three inlet-flow angles

In summary, it was concluded that the shape of the wake profiles at three Reynolds number were similar to each other. However, the width of the wake deficit increased with increasing Reynolds number. This was due to the transition from laminar flow to turbulent flow occurring at a point much nearer to the leading edge. The thickness of the turbulent flow boundary layer increased along the blade length and created a larger wake deficit at the trailing edge. With decreasing incidence angles, the velocity drop at the pressure side was observed to be more severe. The size of the wake deficit was observed to be larger with decreasing incidence angles. There was a persistent (small) departure from periodicity in the two passages.

The turbulence intensity plots for 35 degrees inlet-flow angle are shown in Figure VI.9. The freestream turbulence intensity from the starting point till 0.18 Y/S was less than 2%. From 0.18 Y/S, a small hump extending from 0.18Y/S to 0.23 Y/S was observed on the pressure side before the rapid increase in the turbulence intensity near the blade trailing edge. The small hump was attributed to the pressure side leading edge flow separation. The data for Reynolds number at 800,000 showed a double peak, which corresponded to the location of maximum gradient of the mean flow, whereas the data for the other two flows at lower Reynolds number (625,000 and 750,000) showed a single peak. The turbulence intensity was observed to recover back to freestream past the blade trailing edge toward the suction side. There was no significant correlation observed between turbulence intensity and Reynolds number.

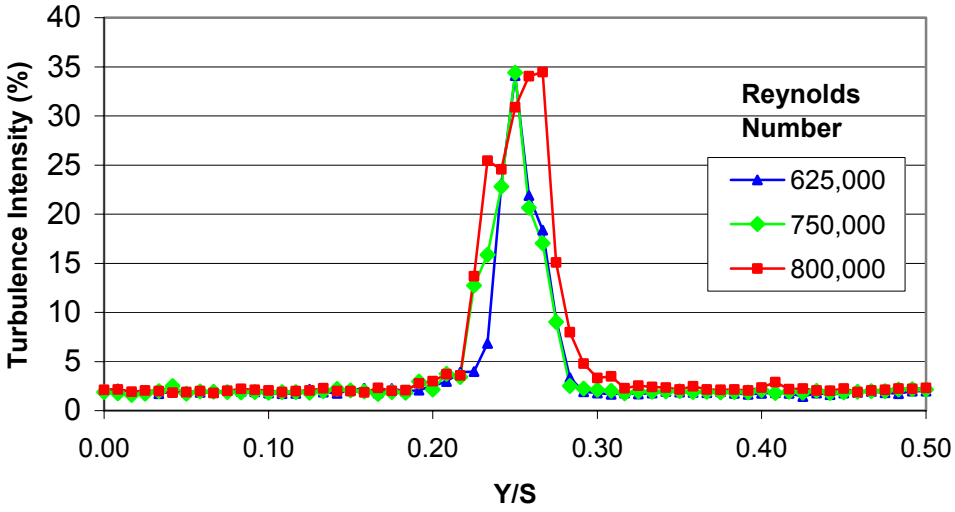

Figure VI.9 Turbulence intensity versus Y/S for inlet-flow angle of 35 degrees

The turbulence intensity plot for 33 degrees inlet-flow angle is shown in Figure VI.10. The turbulence intensity profile for 33 degrees inlet flow angle was similar to those of the 35 degrees inlet flow angle. The significant observation was that the hump, which signifies pressure side flow separation, has grown significantly and it extends from 0.2 Y/S to 0.26Y/S. The data for Reynolds number at 625,000 and 750,000 showed a

double peak, which corresponded to the location of maximum gradient of the mean flow. Mean flow data for Reynolds number at 800,000 showed a single peak.

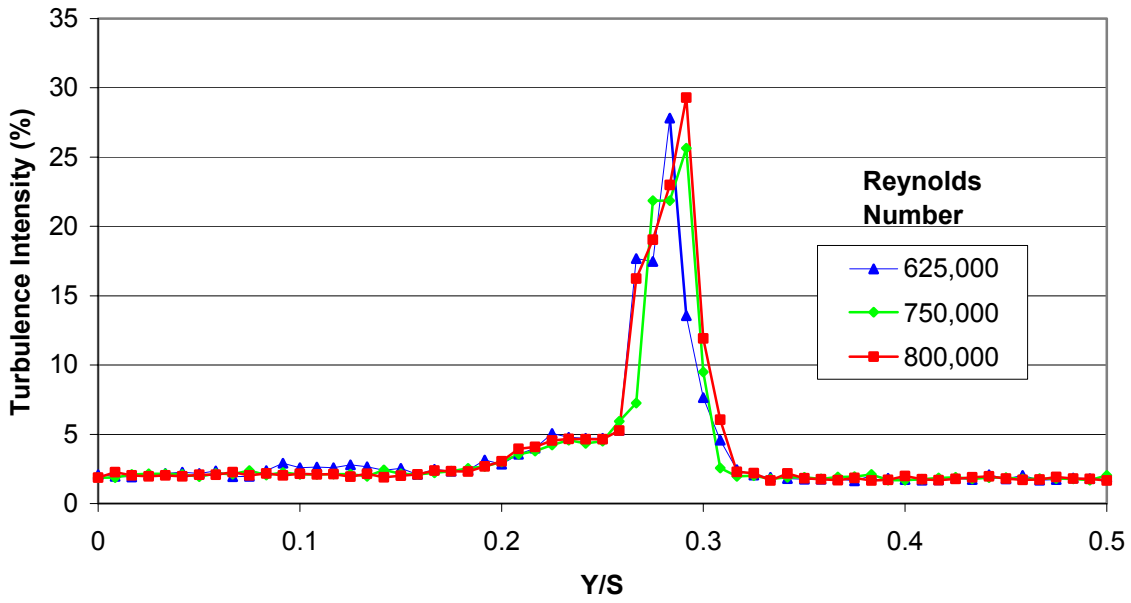

Figure VI.10 Turbulence intensity versus Y/S for inlet-flow angle of 33 degrees

The turbulence intensity plots for 31 degrees inlet-flow angle is shown in Figure VI.11. The turbulence intensity profile for 31 degrees inlet-flow angle was similar to those of the 35 degrees inlet-flow angle. The data for Reynolds number at 800,000 showed a double peak, which corresponded to the location of maximum gradient of the mean flow, whereas the data for two other flows at lower Reynolds number (625,000 and 750,000) showed a single peak. The significant observation was that the hump, which signifies pressure side flow separation, has grown significantly and it extends from 0.15 Y/S to 0.26Y/S.

By combining the turbulence intensity plots at different inlet-flow angle but at a common Reynolds number (i.e. 625,000), as shown in Figure VI.12, the size of the hump, which is associated with leading edge separation, was observed to increase along with decreasing incidence angles.

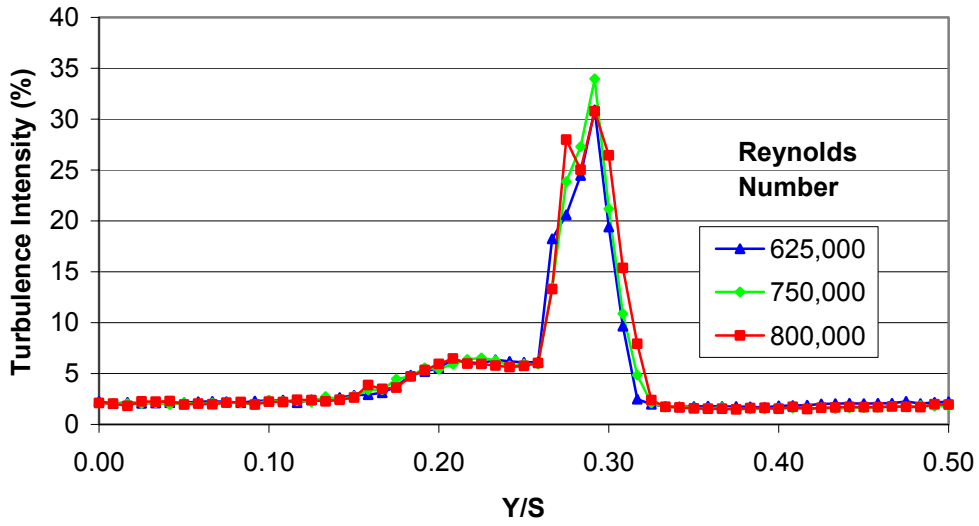

Figure VI.11 Turbulence intensity versus Y/S for inlet-flow angle of 31 degrees

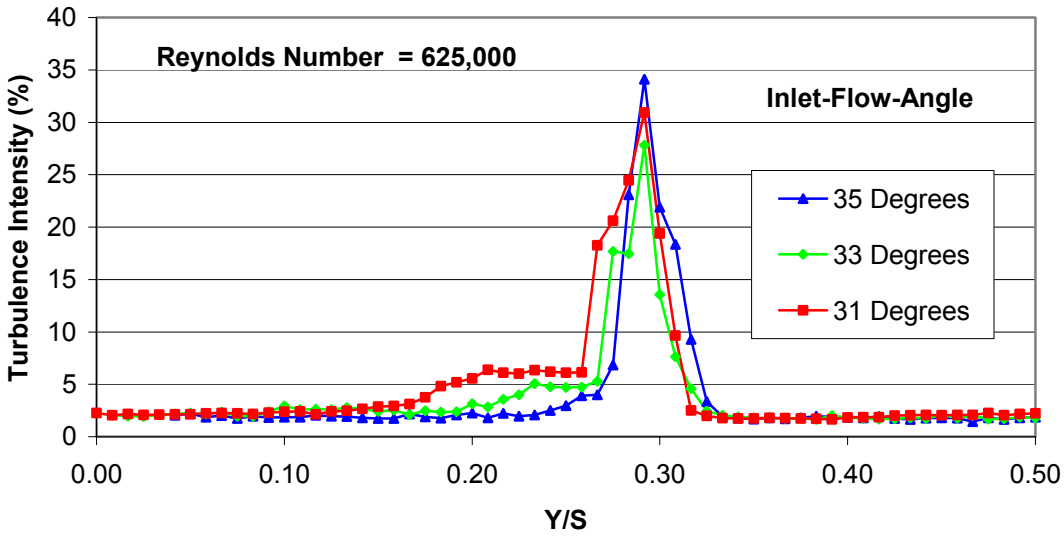

Figure VI.12 Turbulence intensity versus Y/S for three inlet-flow angles

In summary, it was concluded that the turbulence intensity profiles were similar to each other with no significant relationship observed with increasing Reynolds number. The size of the hump, which was associated with leading edge separation, was observed to increase along with decreasing incidence angles. This observation provided evidence that the magnitude of the leading edge separation on the blade's pressure side increased with decreasing incidence angles.

C. STROUHAL NUMBER SURVEY

The data from the wake profile survey were used to characterize the vortex shedding phenomenon at the compressor blade trailing edge. Using the ThermoPro software, the frequency power spectrum plot for each point across the blade passage was generated and analyzed for presence of vortex shedding. A frequency spike on the power spectrum plot indicated the existence of vortex shedding from the blade trailing edge, as shown in figure VI.14. Whereas the power spectrum plot for a probe located at freestream had a gentle power degradation gradient with increasing frequency, as shown in Figure VI.13. After determining the approximate location of vortex shedding on the transverse axis, a Strouhal number survey was conducted by incrementing the Reynolds number. Data samples were taken at two probe locations before and two locations after the location where vortex shedding was detected, for a total of 5 data points. The optimal processing resolution for determining the frequency spike was at 1024 data points, with the application of a Hamming filter. The shedding frequency and Strouhal number were recorded and calculated respectively for each corresponding Reynolds number.

The vortex shedding frequency and Strouhal number versus Reynolds number plot for 35 degrees inlet-flow angle are shown in Figures VI.15 and VI.16 respectively. The frequency spikes were only distinct at a Reynolds number above 350,000. Vortex shedding was observed to occur on the pressure side of the blade only. There was no distinct frequency spike observed on the power spectrum plot for locations on the suction side of the blade. From Figure VI.15, it was observed that the vortex shedding frequency

increased with increase in Reynolds number. The relationship between the vortex shedding frequency and Reynolds number was observed to be nearly linear. From Figure VI.16, it was observed that that mean Strouhal number computed was 0.21 with a standard deviation of 0.02.

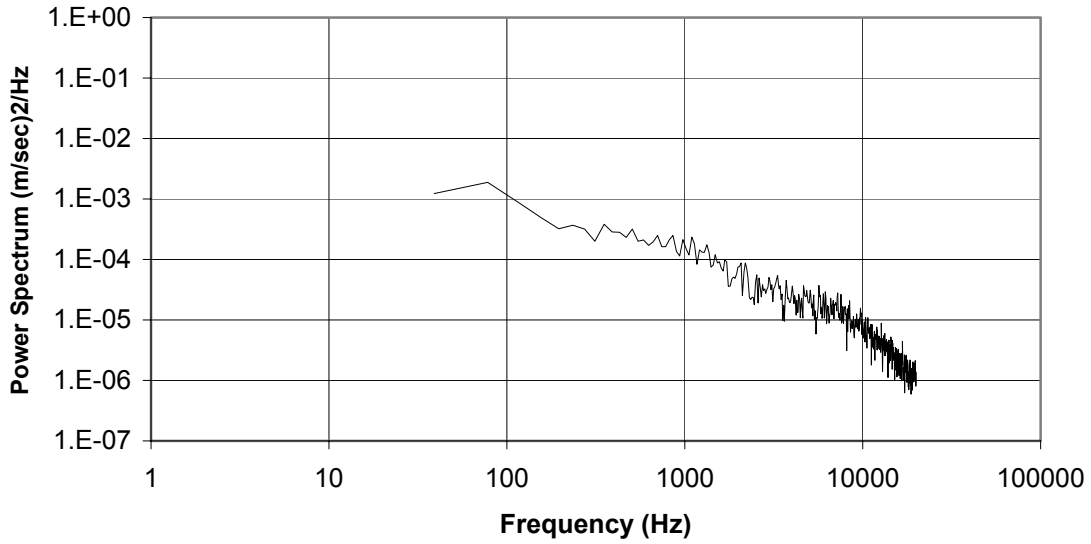

Figure VI.13 Frequency power spectrum plot with probe at freestream

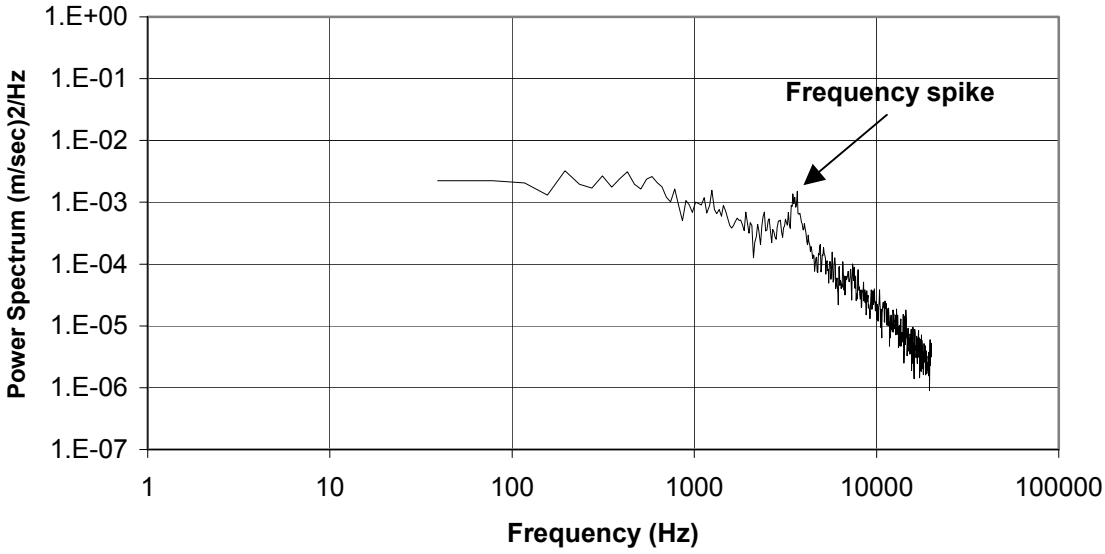

Figure VI.14 Frequency power spectrum plot with probe located near blade trailing edge

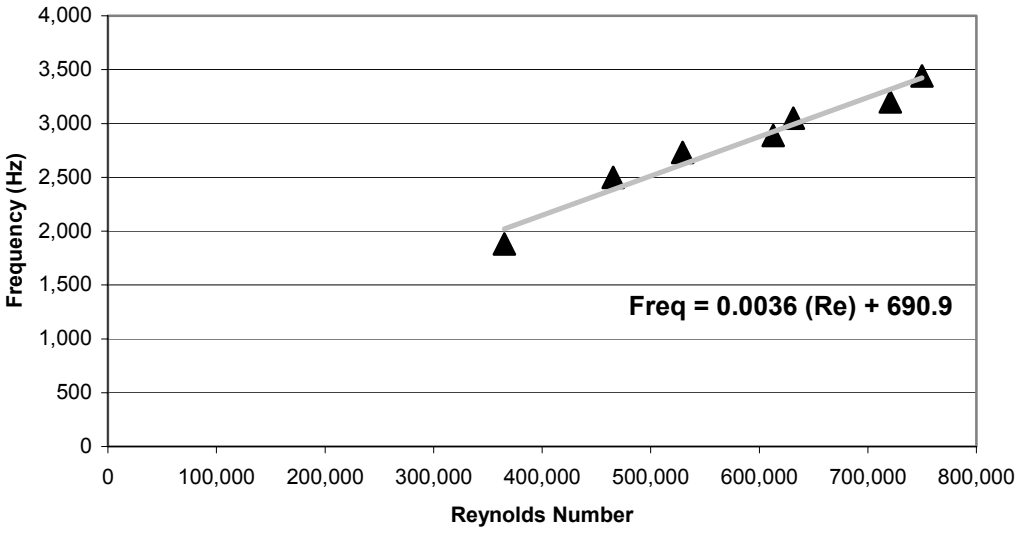

Figure VI.15 Vortex shedding frequency versus Reynolds number for inlet-flow angle of 35 degrees

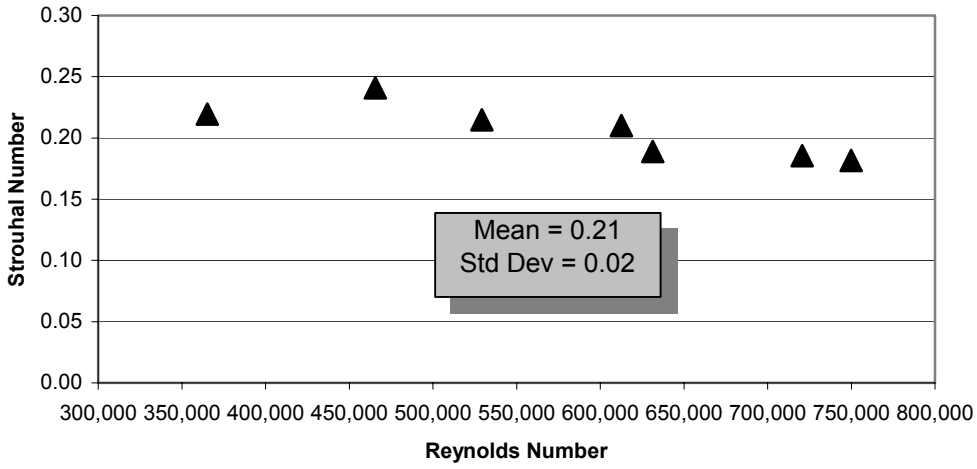

Figure VI.16 Strouhal number versus Reynolds number for inlet-flow angle of 35 degrees

The vortex shedding frequency and Strouhal number versus Reynolds number plot for 33 degrees inlet-flow angle are shown in Figures VI.17 and VI.18 respectively. Similar to 35 degrees inlet-flow angle, the frequency spikes were only distinct at a

Reynolds number above 350,000. Vortex shedding was observed to occur on the pressure side of the blade only. There was no distinct frequency spike observed in the power spectrum plot on the suction side of the blade. From Figure VI.17, it was observed that the relationship between the vortex shedding frequency and Reynolds number was nearly linear. The gradient was observed to be steeper at 0.0052 as compared to 0.0036 for those data collected at 35 degrees inlet-flow angle. From Figure VI.18, it was observed that that the mean Strouhal number was 0.24 with a standard deviation of 0.01. The data points were observed to be more evenly distributed and had less scatter as compared to those computed at 35 degrees inlet-flow angle.

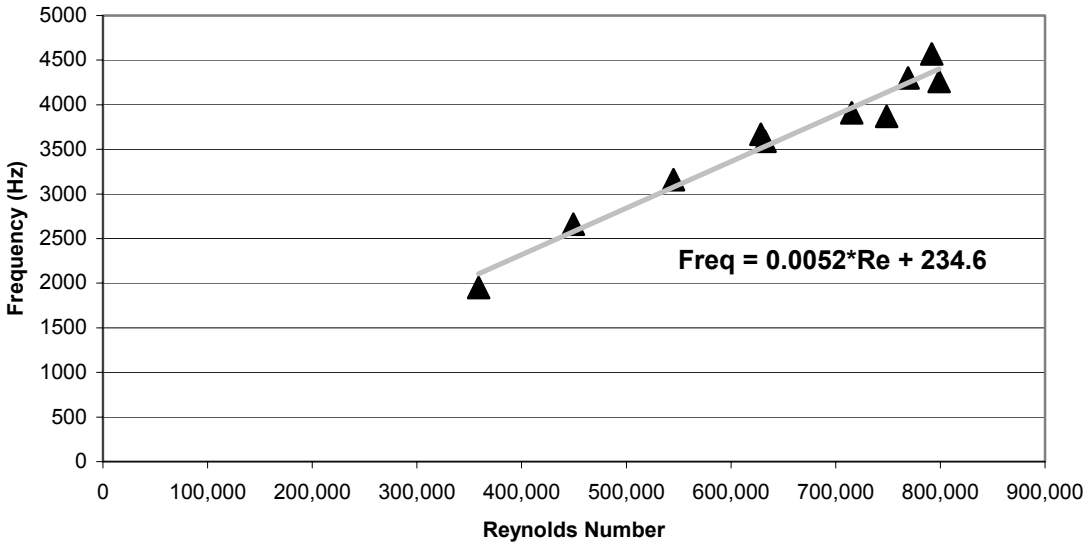

Figure VI.17 Vortex shedding frequency versus Reynolds number for inlet-flow angle of 33 degrees

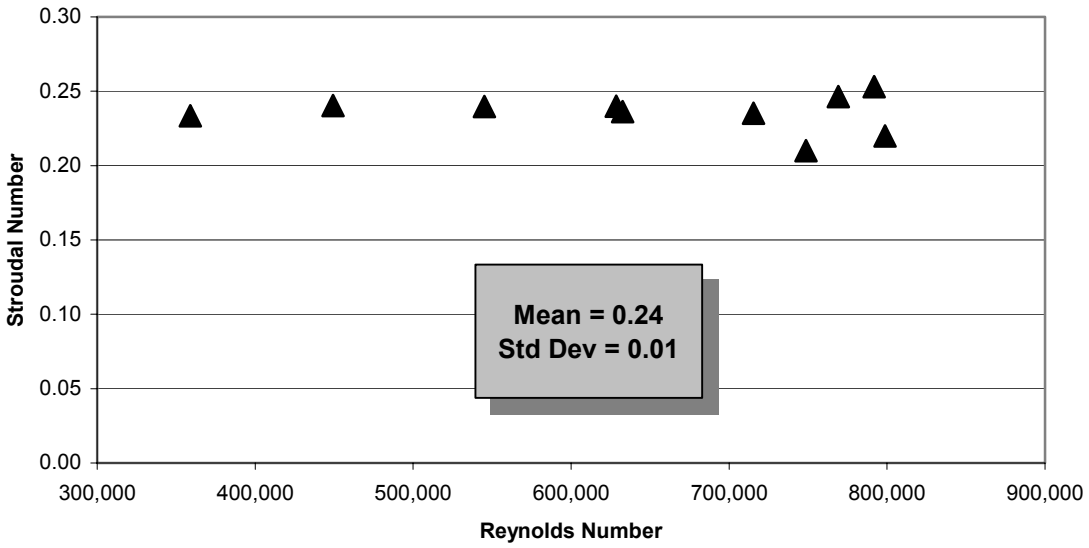

Figure VI.18 Strouhal number versus Reynolds number for inlet-flow angle of 33 degrees

The vortex shedding frequency and Strouhal number versus Reynolds number plot for 31 degrees inlet-flow angle are shown in Figures VI.19 and VI.20 respectively. Only three data points were collected since the initiative to conduct Strouhal number survey was decided after the tunnel was re-configured from 31 degrees to 35 degrees inlet-flow angle. Similar to the other inlet-flow angles, vortex shedding was observed to occur on the pressure side of the blade only. There was no distinct frequency spike observed in the power spectrum plot for on the suction side of the blade. From Figure VI.19, it was observed that the relationship between the vortex shedding frequency and Reynolds number was nearly linear. With limited data points, the gradient was observed to be 0.0043, which was between the values obtained from 35 and 33 degrees inlet-flow-angle. From Figure VI.20, it was observed that that mean Strouhal number computed was 0.19 with a standard deviation of 0.01.

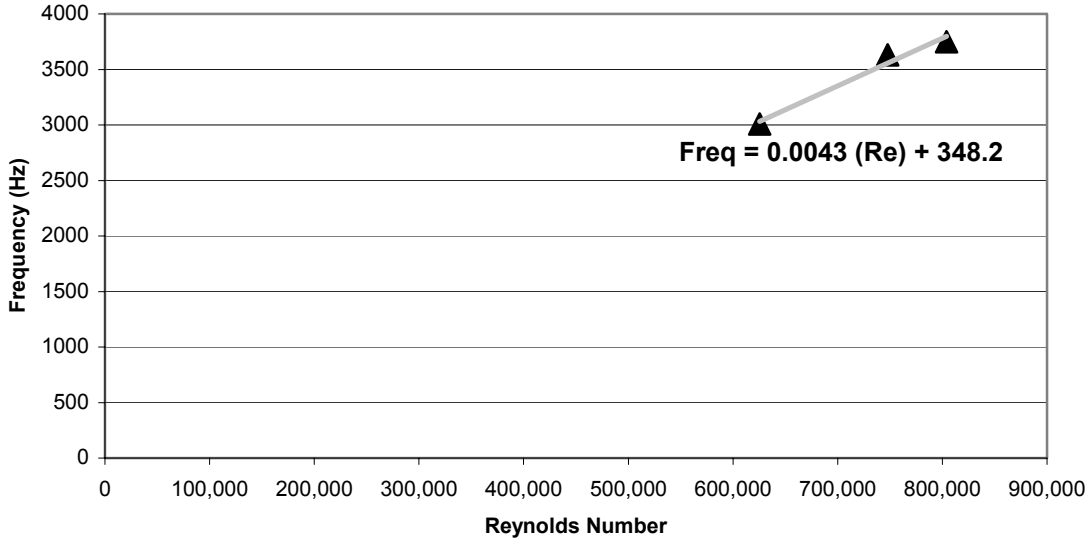

Figure VI.19 Vortex shedding frequency versus Reynolds number for inlet-flow angle of 31 degrees

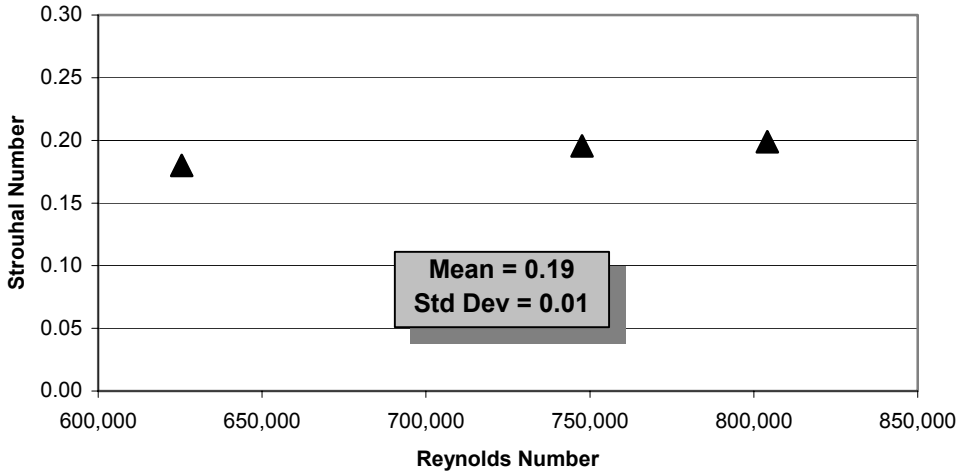

Figure VI.20 Strouhal number versus Reynolds number for inlet-flow angle of 31 degrees

The vortex shedding frequency and Strouhal number versus Reynolds number plot for three inlet-flow angles are shown in Figures VI.21 and VI.22 respectively. From Figure VI.21, the vortex shedding frequency for three inlet-flow angles were nearly linear with increases in Reynolds number. The vortex shedding frequency was observed to be

quite similar at lower Reynolds number (i.e. 450,000 and below) and had a large scatter at higher Reynolds number. In addition, the data seemed to suggest that the magnitude of the vortex shedding frequency had some dependency on the inlet-flow angle. However, due to the limited data collected for 31 degrees inlet-flow angle and the data dispersion at high Reynolds number, the hypothesis could not be fully substantiated.

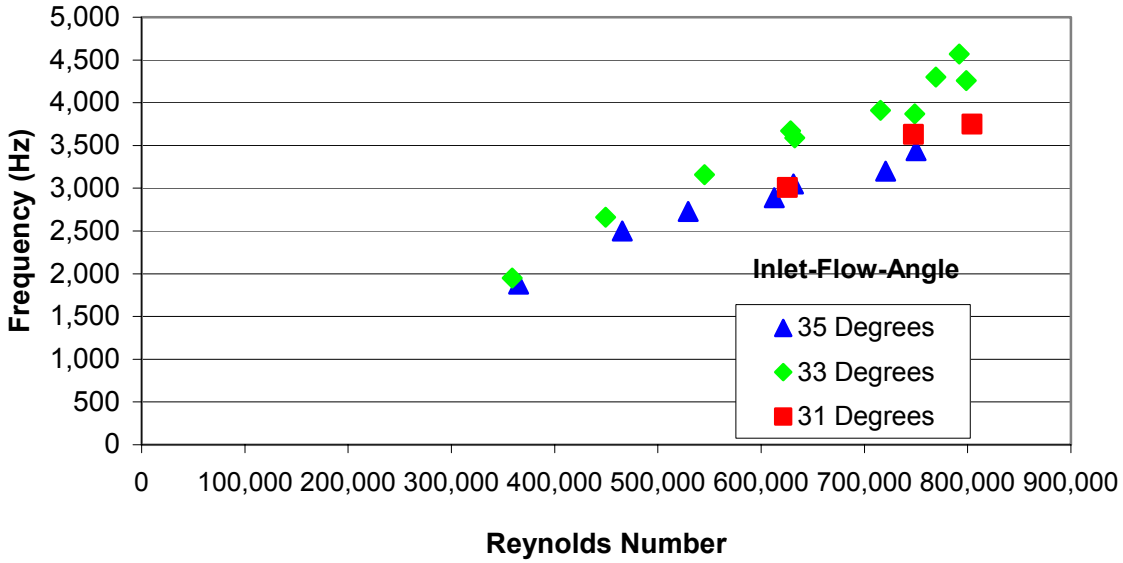

Figure VI.21 Vortex shedding frequency versus Reynolds number for three inlet-flow angles

From Figure VI.22, the Strouhal numbers at 33 and 31 degrees inlet-flow angle were observed to be fairly consistently at about 0.24 and 0.19 respectively. Whereas, the Strouhal number for 35 degrees inlet-flow angle was observed to reduce from 0.22 to 0.18 with corresponding increase in Reynolds number. Similar to the relationship of vortex shedding frequency with Reynolds number, the Strouhal number was observed to be quite similar (about 0.22 to 0.23) at lower Reynolds number (i.e. 450,000 and below) but had large scatter (between 0.18 to 0.25) at higher Reynolds number. For lower Reynolds number, it seemed that a relationship between Strouhal number and angle of incidence could be established. However, due to the limited data collected at 31 degrees inlet-flow angle and the data dispersion at high Reynolds number, the hypothesis could not be fully substantiated.

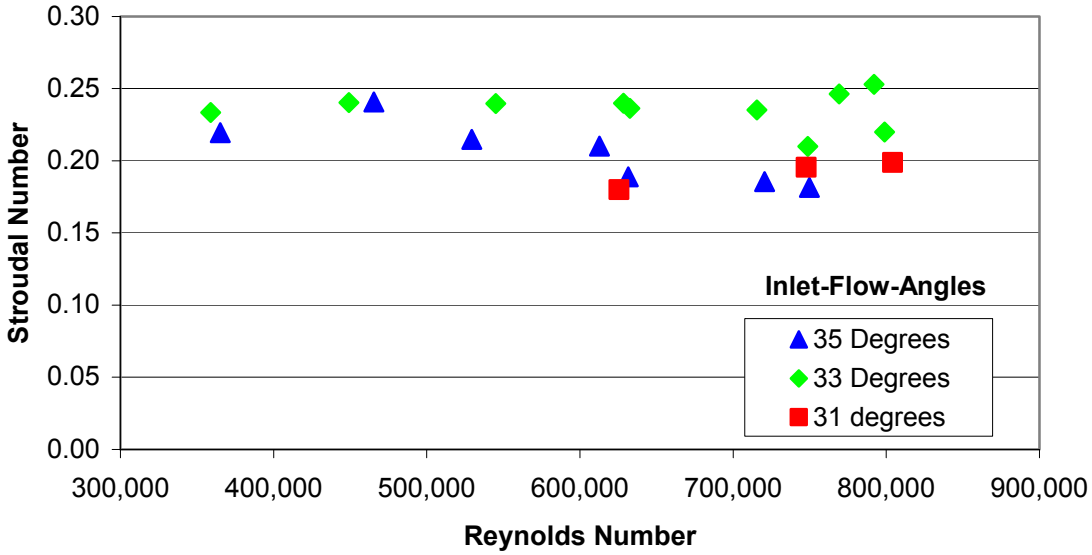

Figure VI.22 Strouhal number versus Reynolds number for three inlet-flow angles

Experimental data of a vortex sheet behind a circular cylinder, (documented by Roshko [Ref. 14] and U.S. Naval Research Laboratory (as presented in a textbook by White [Ref. 15]) showed that the average Strouhal number for Reynolds number between 300,000 to 500,000 was between 0.2 and 0.23. Large data dispersion (between 0.19 to 0.27) was observed as the Reynolds number increased from 500,000 to 800,000.

In summary, the Strouhal number survey has shown that the vortex shedding frequency varied nearly linear with Reynolds number. The vortex shedding frequency was observed to be quite similar at lower Reynolds number (i.e. 450,000 and below) and had a large scatter at higher Reynolds number. The Strouhal number was between 0.22 and 0.24 for low Reynolds number and between 0.18 and 0.25 with increasing Reynolds number. The definitive relationship between vortex shedding frequency and Strouhal number with decreasing incidence angles could not established due to the limited data available.

THIS PAGE INTENTIONALLY LEFT BLANK

V. CONCLUSIONS AND RECOMMENDATIONS

A. CONCLUSIONS

Second-generation controlled-diffusion compressor blade sections, which modeled the midspan section of NASA's stator 67B, were investigated in the LSCWT. The objective of the study was to locate, identify and characterize vortex shedding aft of the blades at three different off-design negative incidence angles, corresponding to inlet-flow angles of 31, 33 and 35 degrees, at Reynolds numbers of 625,000, 750,000 and 800,000.

Blade surface pressure distributions were measured at midspan for each Reynolds number at each inlet-flow angle. A suction-side, laminar-flow separation was found at each inlet-flow angle and low Reynolds number. At higher Reynolds number, the boundary layer underwent transition ahead of the bubble, which energized the velocity profile at the blade surface, and partially suppressed the separation bubble. On the pressure side, the initial pressure spike indicated the existence of a leading edge separation. The size of the leading edge separation bubble and the laminar to turbulent transition region were significantly larger for flows at decreasing incidence angles for all Reynolds numbers.

The wake flow was characterized through hot-wire measurements at midspan, downstream of the compressor blades. The wake velocity profiles were similar in shape, with the size of the wake deficit increasing at higher Reynolds number. This was due to the transition from laminar flow to turbulent flow occurring at a point much nearer to the leading edge. The thickness of the turbulent boundary layer increased along the blade length and created a larger wake deficit at the trailing edge. The velocity drop on the pressure side was observed to be more severe with decreasing incidence angle. In addition, the size of the wake deficit was observed to be larger with decreasing incidence angles.

Conversely, the wake turbulence intensity profiles were similar to each other at all Reynolds number. The maximum turbulence intensity levels that were measured in the wake were in excess of 30%.

Vortex shedding from the leading edge on blade pressure side was documented. The detection of vortex shedding in the wake survey corresponded to the point of maximum gradient in the mean velocity flow and turbulence intensity flow profile. Surveys were conducted at three inlet-flow angles to relate the vortex shedding frequency and Strouhal number to increasing Reynolds number. The Strouhal number survey showed that the relationship between vortex shedding frequency and Reynolds number was nearly linear. The vortex shedding frequency for all incidence angles was observed to be quite similar at lower Reynolds number (i.e. 450,000 and below) and have larger scatter at higher Reynolds number. Similarly, the Strouhal numbers (between 0.23 to 0.24) were observed to be fairly consistent at lower Reynolds number, and to have larger scatter (0.19 to 0.25) at increasing Reynolds number. These observations were consistent with the experimental data of a vortex sheet behind a circular cylinder, as documented by Roshko [Ref. 14] and U.S. Naval Research Laboratory (as presented by White [Ref. 15]). The relationship between vortex shedding frequency and Strouhal number with decreasing incidence angles could not established, due to the limited data available.

B. RECOMMENDATIONS

It is recommended that a new series of Strouhal number surveys be conducted with three repetitive data sets from Reynolds number 300,000 to 800,000 and at 3 inlet flow angles. The three repetitive data sets are required to check for repeatability and to confirm the current observations that both vortex shedding frequency and Strouhal are fairly consistent at lower Reynolds numbers and more scattered as Reynolds number increases beyond 500,000. The data will also aid in establishing the relationship, if any, between the vortex shedding frequency and Strouhal number with decreasing incidence angles. Also, if a more complete data set were obtained, it might be possible to find a logical length scale (which depends on blade angle) and reference velocity (which depends on changing inlet and outlet velocities), which gave a unique variation between Strouhal and Reynolds number at all blade settings.

It is also recommended that an automated data acquisition system and transverse mechanism with a finer resolution be installed. The hotwire probe holder design should also be improved to ensure adequate stiffness during tests at high airflow velocity. The automation of the data acquisition and transverse system will eliminate most of the physical work associated with data collection and aid in improving data collection. A transverse mechanism with finer resolution, together with an improved hotwire probe holder (i.e. increased stiffness), will aid in refining the resolution of the flow profile.

THIS PAGE INTENTIONALLY LEFT BLANK

APPENDIX A: TABLES OF SCANIVALVE PORTS AND CHANNEL ASSIGNMENTS

Scanivalve #1

Blade Pressure Measurements

1	Atmosphere	25	3 Suct. Side
2	Calibration	26	4 Suct. Side
3	Plenum Press	27	5 Suct. Side
4	18 Press side	28	6 Suct. Side
5	17 Press side	29	7 Suct. Side
6	16 Press side	30	8 Suct. Side
7	15 Press side	31	9 Suct. Side
8	14 Press side	32	10 Suct. Side
9	13 Press side	33	11 Suct. Side
10	12 Press side	34	12 Suct. Side
11	11 Press side	35	13 Suct. Side
12	10 Press side	36	14 Suct. Side
13	9 Press side	37	15 Suct. Side
14	8 Press side	38	16 Suct. Side
15	7 Press side	39	17 Suct. Side
16	6 Press side	40	18 Suct. Side
17	5 Press side	41	19 Suct. Side
18	4 Press side	42	20 Suct. Side
19	3 Press side	43	TE
20	2 Press side	44	Blade 8, 1 Suct.
21	1 Press side	45	Blade 8, 2 Suct.
22	LE	46	Blade 8, 3 Suct.
23	1 Suct. Side	47	Blade 8, 4 Suct.
24	2 Suct. Side	48	Blade 8, 5 Suct.

Scanivalve #2

5-hole Probe Measurements

1	Atmosphere	25	Not Used
2	Calibration	26	Not Used
3	Plenum Press	27	Not Used
4	P Wall Static	28	Not Used
5	5-hole P1	29	Not Used
6	5-hole P2	30	Not Used
7	5-hole P3	31	Not Used
8	5-hole P4	32	Not Used
9	5-hole P5	33	Not Used
10	P Prandtl tot	34	Not Used
11	P Prandtl stat	35	Not Used
12	Not Used	36	Not Used
13	Not Used	37	Not Used
14	Not Used	38	Not Used
15	Not Used	39	Not Used
16	Not Used	40	Not Used
17	Not Used	41	Not Used
18	Not Used	42	Not Used
19	Not Used	43	Not Used
20	Not Used	44	Not Used
21	Not Used	45	Not Used
22	Not Used	46	Not Used
23	Not Used	47	Not Used
24	Not Used	48	Not Used

THIS PAGE INTENTIONALLY LEFT BLANK

APPENDIX B: HOT-WIRE ANEMOMETRY CALIBRATION AND OPERATING PROCEDURES

I HOT-WIRE CALIBRATION

1. Record current atmospheric temperature (Ta) and pressure (Pa).

2. To measure the probe resistance, insert shorting probe into probe holder.

Caution

Place cardboard box beneath the probe holder to catch the shorting cable, to prevent shorting probe from dropping into the tunnel

3. At the IFA panel, press [RES MEAS] and check that the [Null Displ] light illuminate. Zero with the operating resistance control knob.

4. Press [RES MEAS] and then press [ENTER].

5. Remove shorting probe and replace with hot-wire probe. Repeat step 3 to 4, except do not press [ENTER] at step 4. Record the resistance value (Ro).

6. Press [OPER RES]. Adjust the operating resistance in probe box.

7. Press [BRIDGE COMP]. Adjust to 115 for 20μm probe or 67 for 10μm probe. Press [RUN].

8. Record no-flow voltage (Eo), which appears next to the channel output (approximately 1.15V).

9. Prepare to start wind tunnel:

   a. Locate window control switches (Qty:4). Open all windows.
   b. Locate main power supply box and switch on the "Power on" switches.
   c. Wait for 30 seconds for tunnel to start up correctly.

10. Locate the pressure control valve and increase the pressure to about 13 psi (as shown in pressure gauge). Hold for 30 seconds. The plenum pressure water manometer display should indicate about 20" to 12" H_2O.

11. Turn cable control knob counterclockwise until [OSC] light illuminate. Turn the knob clockwise until the light goes off. Add another half turn clockwise. Record voltage (Em).

12. Reduce the plenum pressure to zero. Shut down the tunnel from the main power supply box.

13. Switch on the Data Acquisition PC. Double-click the IFA 100 software.

14. Click [COMMUNICATION], [REMOTE], [SEND] and [CLOSE]. Check that the [Local/Remote] switch was correctly set to [Remote].

15. Click [IFA100] and [Monitor]. Check if computer reads correct probe output voltage. {Note: Value displayed by IFA = (Voltage displayed by monitor – Offset value) * Gain}

16. Click [CALIBRATION], [PROBE DATA] and [READ].

17. Enter or alter the parameters on the Calibration-Probe Data screen. Check that [A/D Chan = 1], [IFA Chan = 1], [Probe type = S], [Serial number = filename], Type = W for wire or F for Film] and [Temp Chan = Ext].

18. Click [Gain and Offset]. Enter the low flow (Eo) and high flow (Em) voltage. Click "Calculate" and record the computed "Gain" and "Offset" recommended.

19. To measure the cable resistance, click [Read], [Measure], [Save] and [Close].

20. Check that the Operating resistance (Ro), Offset and Gain value are correct. Select [Cal Method = Acquire E & Type dP].

21. If settings are correct, click [Calibrate]. The Conditions Setup screen will then appears.

22. Check that the [Atm Press = Pa], [Cal Temp= Ta], [Opr Temp = 250C], [Min Vel = 0], [Max Vel = 100 m/s] & [Cal Method = Acquire and type dP].

Note

If the dP Gain display indicates higher values other than 1, click [IFA100}, [dP & Velocity Calculator], adjust dP gain to 1 and click [Close].

23. From the [Acquire Cal Point], enter [10 # points]. Check [Next point = 1], [Yp vel = 1] and [Calibrating = Velocity]. Set [dP] to zero.

24. Press [Acquire]. Select [Nozzle 1]. The first calibration point has been taken at 0" H_2O dP. Check that [Vel = 0].

25. Start up the tunnel as stated in step 9. Increase the throttle pressure from 5 psi to 12 psi (at interval of 1 psi). Enter the dP (in term of H_2O inches) value and click [Acquire]. Record the data at each interval in the following format:

Sample Calibration Sheet

Ta	Pa	Rc	Ro	Rop	Bridge	Eo	Em

Gain	Span	Offset

Plenum Press (psi)	Plenum Press (inch H2O)	Pitot Press (dP) (inch H2O)	Plenum Temp (Degree F)	Voltage (V)	Voltage (RMS)	Velocity (m/s)
0						
5						
6						
7						
8						
9						
10						
11						
12						
13						

King's Law Coefficients

A = _____ B = _____ 1/n = _____

26. After the calibration is completed, click [Next screen], [Curves], [Polynomial], [Plot], [King's Law] and [Plot].

27. Record the King's Law Coefficients. Click [Close] and [Save]. The hotwire anemometry system calibration is completed. The system is ready for data acquisition.

II DATA ACQUISITION

28. Lower the hotwire probe to 1/8" from 4th blade trailing edge.

29 At the PC, click [Acquisition] and [Probe Table]. Click [Get File]. Enter experiment name (up to 8 alphanumeric characters) e.g. CurrentDate.R001. Click [OK].

30 Click [Add Probe]. Select the probe serial number in which the calibration data was stored. Check that the probe data file and the experiment file are in the same directory. Click [OK]. The new experiment name "Filename.RXXXX" should appear in the heading. Check the parameters on the Acquisition – Probe Table screen for correct serial number, operating resistance, gain and offset value, etc.

31. Click [Next screen] and the [Acquisition – Conditions Setup] screen will appear. Enter the current atmosphere pressure (Pa). Check settings [Mode = Graphics], [Low Pass = 100,000], [Rate = 40 KHz], [Size = 8K], [Position X = 0 inch]. When entering the filter setting, click slowly to allow the IFA to respond first before proceeding to the next increment.

32. At the IFA panel, select "Local mode" and press "Output Display". Check for correct no-flow voltage. Check that the IFA is in the "Run Mode". At the PC, click [IFA100] and [Monitor]. Click [Remote] and check that the IFA revert to [Remote].

33. Before proceeding further, check that the transverse counter is set at the initial position (counter = _____).

34. Start up the cascade tunnel and set the plenum pressure at required pressure for data collection.

35. Click on [Next Screen] and the [Realtime Display] screen will appear. Once you are ready to enter data, click [Trigger] and [Close].

36. After a data point is taken, manually transverse the probe by quarter inch (1 inch equivalent to 20 counts). Enter the new X-coordinate. Repeat step 7 and 8 till 61 sets of data at 0.05 inches interval are acquired. Once acquisition is completed, click [Close].

Note

If you encounter problem during data acquisition, select "Local mode" and press "Output Display" at the IFA panel. Check that the IFA is in the "Run Mode". At the PC, click [IFA100] and [Monitor]. Click [Remote] and check that the IFA revert to "Remote". Repeat the last point acquisition.

III POST ANALYSIS

37. Data analysis is performed using the [Post Analysis] menu. Click [Post Analysis] and [Velocity analysis]. Select the acquired raw data files. E.g. CurrentDate.R0001. Click [OK].

38. To begin data analysis, click [Analyze Files]. It will take a few minutes for the PC to analyze the files. Once completed, you may view the data statistics and time history by clicking the [View Statistics] and [Time History] respectively. When done, click [Close].

39. To plot the wake mean velocity profiles, click [Post Analysis] and [Flow Field]. Click [Get Stats Files]. Select the first Stats file e.g. group1.S0001. Click [OK]. Click [Enter] and [Build Flow Field]. Enter the plot filename e.g. group1.plt. Click [OK]. Click [Next Screen] to observe the flow field.

40. To plot the Turbulence Intensity plot, at the [Axis 2], select [Turb Init (%)]. Click [Save] and [Configure]. Observe the generated plot.

41. To obtain the data in spreadsheet format, locate the filename.PRN in the same directory and open the file from Excel. Convert and save the file in Excel format.

THIS PAGE INTENTIONALLY LEFT BLANK

APPENDIX C: BLADE SURFACE MEASUREMENT OPERATING PROCEDURES

I. INITIAL SETUP

1. Open the air supply valve and set the calibration manometer to 10" of water.

2. Start up the tunnel and set to the required inlet velocity. Allow 30 minutes for tunnel to be fully warm-up.

3. Switch on HP75000 Series B VXI-Bus Mainframe and the PC running the HP-VEE software.

4. At the mainframe switchboard, use a cable to connect the calibration console to the digital voltmeter.

5. At scanivalve #1, select channel 1. Adjust the "Zero" control knob till the digital voltmeter reads zero volt.

6. At scanivalve #1, select channel 2. Adjust the "Cal" control knob till the digital voltmeter reads 10 mV.

7. Repeat the step 5 and 6 for scanivalve #2. The system is calibrated for data acquisition.

II. DATA COLLECTION

8. At the PC, double click "Garth Cp" icon.

9. Click the "I/O" tab and select "Instrument manager". Click "Find Instruments". The system will now locate the digital voltmeter and scanivalves connected to the mainframe. Click OK when done.

10. Click "Start". The PC will now prompt you to enter filename to save data. Enter the filename and select scanivalve #1 for Cp survey. The system will automatically acquire and save pressure data from the ports located on the blade surface.

11. Once completed, the system will prompt you to collect another set of data. Click "No". The system will then transfer the recorded data to a spreadsheet. Save the spreadsheet under a new filename "MMDDYY.xls".

12. To collect inlet delta pressure, click "5_hole_scan" icon and repeat step 9 to 11.

THIS PAGE INTENTIONALLY LEFT BLANK

APPENDIX D: LASER-DOPPLER VELOCIMETRY OPERATING PROCEDURES

I. INITIAL SETUP

1. Put up warning signs at main and side entrance. Switch on the warning lights. Lock the main entrance from the outside. Placed a chair at the main entrance from inside the building.

2. Turn on the laser cooling system water supply. Check that the flow pressure is about 20 psia. Check for proper water discharge from the drainage hose.

3. Switch on the circuit breaker located at Panel A # 25.

4. Before activating the laser system, ensure that the current control knob located at the laser power control panel is turn fully anti-clockwise.

5. At the laser power control panel, switch "Main Line" switch to "On" position. Check that the 3 lights next to the switch illuminate accordingly.

6. Turn the "Key control" to "On" position. Check that the 4 lights for "Covers", "Water Tem", "Water Flow" and "Reg Temp" illuminate accordingly.

7. Press "Power On" button. Wait for "Ready" light to illuminate.

8. Press "Laser Start" button. Allow laser to warm up for 15 to 30 minutes.

II. LASER TUNING

9. Locate the laser intensity meter before the transparent panel of the cascade. Switch on the intensity meter.

10. Set laser power to 750 mW using the current control button for coarse adjustment.

11. Translate the laser to locate the blue beam at the center of the intensity meter optical sensor.

12. Tune the laser using the adjustment knobs to get the maximum power reading from intensity meter. Record the maximum power intensity achieved in record book.

13. Repeat the procedures for all four beams.

III. LASER POSITIONING

14. Place laser alignment tool between 3rd and 4th blade. Wear safety goggle before proceeding.

15. Translate the laser in Y direction till 4 beams collate into a very fine spot.

16. Translate the laser (Select "Jog and "Slow" mode for better resolution) in the X and Z direction till the laser spot hit the center of the lower drilled hole of the alignment tool.

17. Look behind the alignment tool to check the 4 beams for even intensity.

18. Press "Relative Home" for three-axis on the control box.

19. From the PC, double click "FFW16".

20. Go to "Transverse" and "Manual". Check the figures in the respective axis are all zeros. Press "Rel Home" to set the current position as relative home.

21. Enter " –87.653" in X-direction and "42.750" in the Z-direction. This should move the laser to the first survey location, with 2 laser beams just touching the blade. Press "Rel Home" to set the current position as relative home.

IV. DATA COLLECTION

22. From the PC, double click "FFW16".

    a. Click "File" and "New Experiment". Enter "MMDDYY#.exp".

    b. Click "File", "Transverse File" and "New". Enter "MMDDYY#.trv".

    c. Enter the transverse matrix (just like Excel spreadsheet). Save file once updated.

23. Click "Setup" and "Experiment". Set data path. Set Start file # (usually 1) and number of file to be run (usually 25). Set "Time out" between 10 to 30 secs depending on the rate of data acquired and amount of seeding input. Set "Data points" (usually 1 for 1000 points). Save experiment.

24. Click "Options" and "TSI Hardware". Press "Search for address". Check that "default 6260" appears and click "Close".

25. Click "Experiment" tab. Set following parameters:
    a. Data Path: C:\ffw16\data
    b. Starting File Number: 1 (as desired)

c. Data point per file: 1000 points
d. Time out: 300 secs
e. Positions per run: 1
f. Start Run at position:1

26. Click “Instruments” tab. Set the following parameters:
    a. Measurement: Velocity
    b. Processor Type: IFA755
    c: Processor COM Port: COM 1
    d. Channels: 2
    e. Traverse Type: ampro.dll
    f. Traverse COM Port: COM 2
    g. Color Link: Remote

27. Click “Laser Optics” tab. Set the following parameters:
    a. Channel 1: Beam Spacing: 50 mm
       Focal Length: 350 mm
       Laser Wavelength: 514.5 nm
    b. Channel 2: Beam Spacing: 50 mm
       Focal Length: 350.00 mm
       Laser Wavelength 488.0 nm
    c. Under [CALC] button, select FRINGE SPACING, then Click [CALC]

28. Disregard APV Xmit, APV Recv, Datalink and Matrix tabs.

29. Click “Setup Window”, “Instruments “Tab. Click [Connect].

30. Click “Views”, “LDV” View Window. Select [Blue], [Green] and [TAB] icons.

31. Click “Control View”. Set the following parameters:
    a. Processor Setup tab:
       Mode: Random or Coincidence
       Time Between Data: Time Stamp
       Other options deselected
    b. Processor Control tab:
       Frequency Range: Search All (This action should
       Yield a frequency range of 5Mhz to 30Mhz on channel 1 & 2
       Operating parameters: Normal
       Min. threshold: Channel 1 = 50 & Channel 2 = 10
       Color Link tab:
       Shifter: 1 and 2
       Frequency shift: 5 Mhz
       Select flow direction right to left :
       For Shifter 1, PMT1 = 1000
       For Shifter 2, PMT1 = 1800

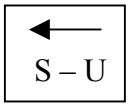

32. Start wind tunnel and set to 12" water plenum pressure. To start seeding, turn air pressure (Air LPM) fully clockwise first and half a turn anti-clockwise. Set the angular dial to zero degree.

33. Select the "Green light" icon to begin data collection. Look at the LDV view to check for rate and uniform data collection for both blue and green channel.

34. If data flow looks acceptable, select the "Red light" icon to stop.

35. Click "Options" and "Start data collection". The software will now initiate data collection from the first point as stated in the transverse file. It will automatically move to the next point once 1000 samples are collected.

36. Move the angular dial by one or two degrees anti-clockwise if the rate of data collection is too slow. For optimal seeding with span travel, adjust the dial for a maximum of 6 degrees anti-clockwise.

Note

If data collection takes too long, time out will cut off the data collection for that point. Check that the Perspex glass is not dirty. Attempt data collection again. If problem persist, re-program the transverse file to skip that specific point by 1 or 2 mm.

V. DATA PROCESSING

37. Click "Statistics", "Run Options", select the raw data file for the experiment. Click [OK].

38. Click "Statistics", " Cumulative Results" and "Extract All". At the spreadsheet, right click the mouse button and save the data file in spreadsheet format for further processing.

APPENDIX E: TABULATED DATA FOR HOT-WIRE WAKE SURVEY

Reynolds 625,000 @ IFA 35 degrees

Ambient Temp = 65F **Plenum Press = 12" H_2O** **Delta Press = 13.1" H_2O**
V ref = 72.63 m/s **Reynolds = 631,444**

Y/S	Umean /Vref	U Ti (%)		Y/S	Umean /Vref	U Ti (%)
0.000	0.896	2.052		0.258	0.441	21.883
0.008	0.889	2.211		0.267	0.493	18.366
0.017	0.892	1.870		0.275	0.737	9.270
0.025	0.886	2.000		0.283	0.909	3.355
0.033	0.887	1.727		0.292	0.930	1.926
0.042	0.879	1.961		0.300	0.936	1.779
0.050	0.888	1.847		0.308	0.945	1.674
0.058	0.879	1.853		0.317	0.932	1.805
0.067	0.888	1.868		0.325	0.939	1.705
0.075	0.888	2.059		0.333	0.945	1.797
0.083	0.878	1.951		0.342	0.938	1.949
0.092	0.872	1.911		0.350	0.955	1.886
0.100	0.876	1.788		0.358	0.948	1.844
0.108	0.887	1.734		0.367	0.950	1.808
0.117	0.887	1.752		0.375	0.952	1.926
0.125	0.898	2.172		0.383	0.942	1.750
0.133	0.883	1.898		0.392	0.947	1.663
0.142	0.882	1.764		0.400	0.954	1.758
0.150	0.884	2.089		0.408	0.948	1.812
0.158	0.889	2.272		0.417	0.950	1.768
0.167	0.881	1.795		0.425	0.960	1.442
0.175	0.894	2.241		0.433	0.960	1.807
0.183	0.897	1.955		0.442	0.963	1.640
0.192	0.902	2.074		0.450	0.961	1.795
0.200	0.901	2.516		0.458	0.963	1.855
0.208	0.900	2.972		0.467	0.957	1.966
0.217	0.889	3.896		0.475	0.951	1.824
0.225	0.886	3.987		0.483	0.952	1.742
0.233	0.860	6.845		0.492	0.952	1.992
0.242	0.508	23.087		0.500	0.962	1.978
0.250	0.269	34.100				

Reynolds 750,000 @ IFA 35 degrees

Ambient Temp = 70F **Plenum Press = 17" H_2O** **Delta Press = 18.45" H_2O**
V ref = 86.25 m/s **Reynolds = 749,879**

Y/S	Umean /Vref	U Ti (%)		Y/S	Umean /Vref	U Ti (%)
0.000	0.862	1.878		0.258	0.513	20.655
0.008	0.860	1.772		0.267	0.561	17.035
0.017	0.867	1.602		0.275	0.808	9.014
0.025	0.868	1.734		0.283	0.934	2.519
0.033	0.869	2.002		0.292	0.939	2.259
0.042	0.869	2.513		0.300	0.934	2.110
0.050	0.863	1.712		0.308	0.940	2.007
0.058	0.852	1.956		0.317	0.943	1.755
0.067	0.854	1.906		0.325	0.939	1.942
0.075	0.856	1.887		0.333	0.937	1.910
0.083	0.863	1.869		0.342	0.932	1.955
0.092	0.862	1.885		0.350	0.938	1.978
0.100	0.853	1.817		0.358	0.938	1.873
0.108	0.850	1.887		0.367	0.939	1.921
0.117	0.861	1.889		0.375	0.939	1.843
0.125	0.860	1.825		0.383	0.933	1.891
0.133	0.861	1.981		0.392	0.946	1.871
0.142	0.859	2.228		0.400	0.951	2.088
0.150	0.868	2.066		0.408	0.934	1.784
0.158	0.872	1.947		0.417	0.943	1.917
0.167	0.861	1.702		0.425	0.943	1.808
0.175	0.877	1.874		0.433	0.940	2.030
0.183	0.873	1.837		0.442	0.948	1.782
0.192	0.882	2.955		0.450	0.933	1.853
0.200	0.886	2.139		0.458	0.944	1.922
0.208	0.898	3.756		0.467	0.941	1.987
0.217	0.879	3.430		0.475	0.938	1.972
0.225	0.700	12.728		0.483	0.937	2.163
0.233	0.605	15.848		0.492	0.941	2.180
0.242	0.219	22.793		0.500	0.932	2.147
0.250	0.191	34.400				

Reynolds 800,000 @ IFA 35 degrees

Ambient Temp = 70F **Plenum Press = 19.4" H_2O** **Delta Press = 21.4" H_2O**
V ref = 92.47 m/s **Reynolds = 803,953**

Y/S	Umean /Vref	U Ti (%)		Y/S	Umean /Vref	U Ti (%)
0.000	0.872	2.111		0.258	0.202	34.029
0.008	0.874	2.146		0.267	0.298	34.474
0.017	0.878	1.908		0.275	0.698	15.077
0.025	0.871	2.051		0.283	0.884	7.980
0.033	0.874	1.974		0.292	0.954	4.803
0.042	0.870	1.809		0.300	0.957	3.306
0.050	0.876	1.896		0.308	0.963	3.486
0.058	0.872	1.995		0.317	0.953	2.284
0.067	0.866	1.777		0.325	0.952	2.533
0.075	0.866	2.029		0.333	0.946	2.418
0.083	0.876	2.220		0.342	0.949	2.341
0.092	0.873	2.121		0.350	0.947	2.152
0.100	0.867	2.043		0.358	0.949	2.477
0.108	0.866	1.904		0.367	0.950	2.152
0.117	0.866	1.977		0.375	0.946	2.134
0.125	0.871	2.040		0.383	0.949	2.158
0.133	0.884	2.273		0.392	0.955	2.036
0.142	0.881	1.983		0.400	0.959	2.331
0.150	0.880	1.977		0.408	0.954	2.903
0.158	0.879	1.859		0.417	0.953	2.175
0.167	0.890	2.297		0.425	0.948	2.232
0.175	0.890	2.011		0.433	0.953	2.052
0.183	0.892	2.073		0.442	0.951	2.017
0.192	0.899	2.757		0.450	0.953	2.242
0.200	0.910	2.994		0.458	0.945	1.894
0.208	0.898	3.724		0.467	0.953	2.061
0.217	0.903	3.576		0.475	0.954	2.125
0.225	0.713	13.677		0.483	0.944	2.238
0.233	0.199	25.453		0.492	0.951	2.213
0.242	0.193	24.549		0.500	0.955	2.319
0.250	0.195	30.873				

Reynolds 625,000 @ IFA 33 degrees

Ambient Temp = 64F **Plenum Press = 12.6" H_2O** **Delta Press = 13" H_2O**
V ref = 72.28 m/s **Reynolds = 628,470**

Y/S	Umean /Vref	U Ti (%)		Y/S	Umean /Vref	U Ti (%)
0.000	0.906	2.073		0.258	0.862	5.281
0.008	0.899	1.965		0.267	0.580	17.677
0.017	0.894	1.915		0.275	0.246	17.470
0.025	0.900	2.089		0.283	0.233	27.819
0.033	0.890	2.183		0.292	0.601	13.569
0.042	0.888	2.271		0.300	0.781	7.645
0.050	0.890	2.160		0.308	0.880	4.583
0.058	0.896	2.350		0.317	0.930	2.438
0.067	0.884	1.952		0.325	0.930	2.060
0.075	0.885	1.961		0.333	0.927	1.899
0.083	0.883	2.388		0.342	0.925	1.799
0.092	0.887	2.919		0.350	0.935	1.766
0.100	0.891	2.587		0.358	0.929	1.746
0.108	0.883	2.623		0.367	0.927	1.771
0.117	0.872	2.595		0.375	0.924	1.647
0.125	0.873	2.786		0.383	0.938	2.017
0.133	0.871	2.649		0.392	0.926	1.833
0.142	0.864	2.406		0.400	0.920	1.740
0.150	0.887	2.541		0.408	0.933	1.692
0.158	0.864	2.097		0.417	0.940	1.704
0.167	0.872	2.473		0.425	0.932	1.814
0.175	0.864	2.337		0.433	0.935	1.741
0.183	0.869	2.396		0.442	0.946	2.086
0.192	0.885	3.140		0.450	0.936	1.773
0.200	0.868	2.834		0.458	0.935	2.026
0.208	0.865	3.561		0.467	0.933	1.688
0.217	0.856	3.992		0.475	0.941	1.722
0.225	0.855	5.069		0.483	0.935	1.848
0.233	0.849	4.778		0.492	0.945	1.793
0.242	0.851	4.709		0.500	0.937	1.903
0.250	0.853	4.719				

Reynolds 750,000 @ IFA 33 degrees

Ambient Temp = 67F **Plenum Press = 17.6" H_2O** **Delta Press = 18.5" H_2O**
V ref = 86.12 m/s **Reynolds = 748,739**

Y/S	Umean /Vref	U Ti (%)		Y/S	Umean /Vref	U Ti (%)
0.000	0.917	1.863		0.258	0.861	5.930
0.008	0.916	1.877		0.267	0.847	7.252
0.017	0.914	2.103		0.275	0.223	21.862
0.025	0.907	2.143		0.283	0.221	21.856
0.033	0.908	2.150		0.292	0.390	25.641
0.042	0.902	2.112		0.300	0.761	9.491
0.050	0.899	1.952		0.308	0.939	2.570
0.058	0.900	2.182		0.317	0.941	1.971
0.067	0.899	2.130		0.325	0.942	2.021
0.075	0.897	2.368		0.333	0.946	1.772
0.083	0.893	2.049		0.342	0.935	1.888
0.092	0.897	2.239		0.350	0.945	1.903
0.100	0.889	2.099		0.358	0.940	1.769
0.108	0.882	2.107		0.367	0.952	1.909
0.117	0.885	2.118		0.375	0.935	1.943
0.125	0.895	2.124		0.383	0.949	2.105
0.133	0.884	1.965		0.392	0.938	1.698
0.142	0.887	2.425		0.400	0.936	1.695
0.150	0.872	2.149		0.408	0.941	1.763
0.158	0.873	2.095		0.417	0.949	1.849
0.167	0.883	2.212		0.425	0.946	1.890
0.175	0.875	2.329		0.433	0.934	1.769
0.183	0.878	2.550		0.442	0.946	1.869
0.192	0.873	2.669		0.450	0.940	1.872
0.200	0.870	3.003		0.458	0.946	1.790
0.208	0.878	3.563		0.467	0.942	1.807
0.217	0.869	3.795		0.475	0.945	1.804
0.225	0.859	4.219		0.483	0.939	1.768
0.233	0.859	4.581		0.492	0.940	1.685
0.242	0.855	4.350		0.500	0.944	2.027
0.250	0.863	4.504				

Reynolds 800,000 @ IFA 33 degrees

Ambient Temp = 69F **Plenum Press = 20.3" H_2O** **Delta Press = 21.4" H_2O**
V ref = 92.59 m/s **Reynolds = 805,000**

Y/S	Umean /Vref	U Ti (%)		Y/S	Umean /Vref	U Ti (%)
0.000	0.916	1.871		0.258	0.854	5.262
0.008	0.904	2.274		0.267	0.636	16.251
0.017	0.910	2.041		0.275	0.234	19.031
0.025	0.901	1.974		0.283	0.217	22.980
0.033	0.907	2.024		0.292	0.358	29.294
0.042	0.904	1.971		0.300	0.672	11.911
0.050	0.891	2.080		0.308	0.848	6.042
0.058	0.884	2.070		0.317	0.927	2.286
0.067	0.893	2.265		0.325	0.939	2.204
0.075	0.887	2.040		0.333	0.928	1.655
0.083	0.878	2.173		0.342	0.939	2.171
0.092	0.881	2.039		0.350	0.928	1.831
0.100	0.877	2.144		0.358	0.932	1.753
0.108	0.871	2.091		0.367	0.933	1.684
0.117	0.877	2.135		0.375	0.942	1.839
0.125	0.866	1.942		0.383	0.931	1.661
0.133	0.876	2.149		0.392	0.933	1.721
0.142	0.859	1.892		0.400	0.933	1.982
0.150	0.869	2.018		0.408	0.940	1.761
0.158	0.871	2.098		0.417	0.935	1.685
0.167	0.871	2.371		0.425	0.938	1.776
0.175	0.865	2.339		0.433	0.938	1.896
0.183	0.862	2.307		0.442	0.937	1.967
0.200	0.867	2.677		0.450	0.939	1.809
0.208	0.860	3.060		0.458	0.940	1.708
0.217	0.861	3.944		0.467	0.950	1.744
0.225	0.855	4.093		0.475	0.943	1.924
0.233	0.847	4.545		0.483	0.946	1.811
0.242	0.843	4.678		0.492	0.951	1.772
0.250	0.846	4.636		0.500	0.944	1.658

Reynolds 625,000 @ IFA 31 degrees

Ambient Temp = 74F **Plenum Press = 12.5" H_2O** **Delta Press = 12.7" H_2O**
V ref = 71.942 m/s **Reynolds = 625,465**

Y/S	Umean /Vref	U Ti (%)		Y/S	Umean /Vref	U Ti (%)
0.000	0.908	2.264		0.258	0.930	6.145
0.008	0.900	2.044		0.267	0.633	18.254
0.017	0.908	2.167		0.275	0.228	20.597
0.025	0.905	2.090		0.283	0.215	24.460
0.033	0.900	2.104		0.292	0.298	30.925
0.042	0.904	2.151		0.300	0.555	19.394
0.050	0.910	2.126		0.308	0.826	9.655
0.058	0.913	2.243		0.317	0.996	2.496
0.067	0.914	2.259		0.325	1.014	1.990
0.075	0.908	2.233		0.333	1.001	1.769
0.083	0.912	2.154		0.342	1.002	1.734
0.092	0.912	2.282		0.350	1.000	1.754
0.100	0.909	2.369		0.358	1.004	1.789
0.108	0.917	2.399		0.367	1.009	1.765
0.117	0.922	2.146		0.375	1.003	1.753
0.125	0.917	2.422		0.383	1.005	1.725
0.133	0.917	2.486		0.392	1.008	1.659
0.142	0.917	2.645		0.400	1.009	1.835
0.150	0.926	2.855		0.408	1.012	1.865
0.158	0.918	2.931		0.417	1.000	1.878
0.167	0.922	3.108		0.425	1.006	2.007
0.175	0.925	3.747		0.433	1.013	2.058
0.183	0.923	4.838		0.442	1.010	2.079
0.192	0.912	5.193		0.450	1.008	2.054
0.200	0.903	5.563		0.458	1.013	2.065
0.208	0.902	6.380		0.467	1.006	2.076
0.217	0.909	6.115		0.475	1.012	2.269
0.225	0.908	6.007		0.483	1.010	2.035
0.233	0.921	6.366		0.492	1.030	2.167
0.242	0.914	6.191		0.500	1.024	2.240
0.250	0.911	6.104				

Reynolds 750,000 @ IFA 31 degrees

Ambient Temp = 71F **Plenum Press = 18.5" H_2O** **Delta Press = 18.2" H_2O**
V ref = 85.991 m/s **Reynolds = 747,628**

Y/S	Umean /Vref	U Ti (%)		Y/S	Umean /Vref	U Ti (%)
0.000	0.880	2.094		0.258	0.864	5.913
0.008	0.889	2.082		0.267	0.721	13.428
0.017	0.878	2.039		0.275	0.212	23.856
0.025	0.866	2.038		0.283	0.182	27.289
0.033	0.869	2.114		0.292	0.210	33.957
0.042	0.869	1.942		0.300	0.445	21.204
0.050	0.865	2.153		0.308	0.685	10.891
0.058	0.877	2.019		0.317	0.890	4.848
0.067	0.867	2.094		0.325	0.940	2.092
0.075	0.862	2.153		0.333	0.949	1.684
0.083	0.863	2.119		0.342	0.945	1.725
0.092	0.853	1.984		0.350	0.941	1.620
0.100	0.860	2.393		0.358	0.942	1.582
0.108	0.861	2.254		0.367	0.943	1.674
0.117	0.850	2.336		0.375	0.939	1.494
0.125	0.870	2.200		0.383	0.937	1.539
0.133	0.857	2.741		0.392	0.945	1.523
0.142	0.871	2.458		0.400	0.940	1.589
0.150	0.862	2.765		0.408	0.948	1.603
0.158	0.866	3.393		0.417	0.944	1.536
0.167	0.870	3.381		0.425	0.934	1.648
0.175	0.869	4.452		0.433	0.934	1.529
0.183	0.869	4.720		0.442	0.934	1.641
0.192	0.859	5.565		0.450	0.933	1.645
0.200	0.862	5.447		0.458	0.939	1.665
0.208	0.855	5.919		0.467	0.945	1.778
0.217	0.861	6.399		0.475	0.940	1.715
0.225	0.853	6.541		0.483	0.947	1.841
0.233	0.858	6.296		0.492	0.942	1.795
0.242	0.858	5.753		0.500	0.954	1.801
0.250	0.865	5.953				

Reynolds 800,000 @ IFA 31 degrees

Ambient Temp = 75F **Plenum Press = 20.5" H_2O** **Delta Press = 21.1" H_2O**
V ref = 92.49 m/s **Reynolds = 804,088**

Y/S	Umean /Vref	U Ti (%)		Y/S	Umean /Vref	U Ti (%)
0.000	0.860	2.122		0.258	0.839	6.029
0.008	0.864	2.052		0.267	0.698	13.296
0.017	0.854	1.837		0.275	0.247	27.975
0.025	0.848	2.250		0.283	0.185	25.019
0.033	0.854	2.238		0.292	0.174	30.776
0.042	0.857	2.290		0.300	0.339	26.434
0.050	0.850	1.935		0.308	0.570	15.375
0.058	0.856	2.040		0.317	0.797	7.936
0.067	0.851	1.983		0.325	0.921	2.377
0.075	0.850	2.123		0.333	0.915	1.738
0.083	0.852	2.213		0.342	0.916	1.670
0.092	0.851	1.948		0.350	0.913	1.582
0.100	0.850	2.232		0.358	0.915	1.538
0.108	0.850	2.214		0.367	0.908	1.534
0.117	0.848	2.436		0.375	0.904	1.487
0.125	0.859	2.380		0.383	0.909	1.588
0.133	0.843	2.271		0.392	0.909	1.642
0.142	0.864	2.420		0.400	0.907	1.554
0.150	0.859	2.628		0.408	0.908	1.724
0.158	0.857	3.882		0.417	0.904	1.500
0.167	0.867	3.483		0.425	0.911	1.639
0.175	0.862	3.626		0.433	0.905	1.663
0.183	0.854	4.711		0.442	0.909	1.723
0.192	0.840	5.342		0.450	0.914	1.713
0.200	0.848	5.949		0.458	0.911	1.713
0.208	0.837	6.466		0.467	0.916	1.761
0.217	0.832	5.970		0.475	0.909	1.742
0.225	0.822	5.936		0.483	0.906	1.711
0.233	0.831	5.774		0.492	0.924	1.968
0.242	0.835	5.636		0.500	0.913	1.963
0.250	0.837	5.745				

THIS PAGE INTENTIONALLY LEFT BLANK

APPENDIX F: FREQUENCY SPECTRUM PLOTS FOR STROUHAL NUMBER SURVEY

Strouhal Number Survey @ IFA 35 degrees
Ambient Temp = 62F **Plenum Press = 4.1" H_2O** **Delta Press = 4.3" H_2O**
V ref = 42 m/s **Reynolds = 365,159** **Point number = 28**

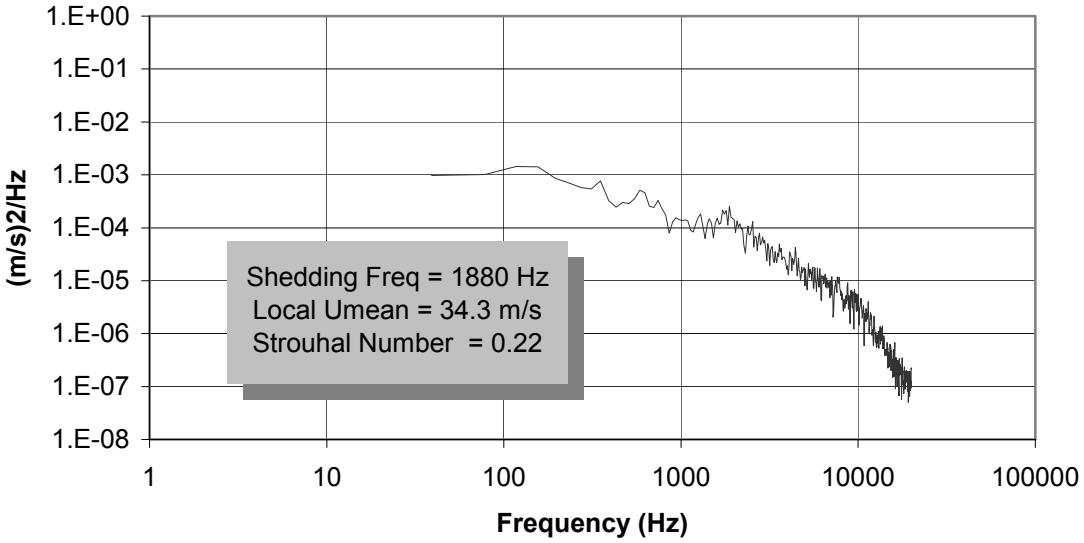

Strouhal Number Survey @ IFA 35 degrees

Ambient Temp = 62F	**Plenum Press = 6.6" H_2O**	**Delta Press = 7" H_2O**
V ref = 53.5 m/s	**Reynolds = 465,513**	**Point number = 28**

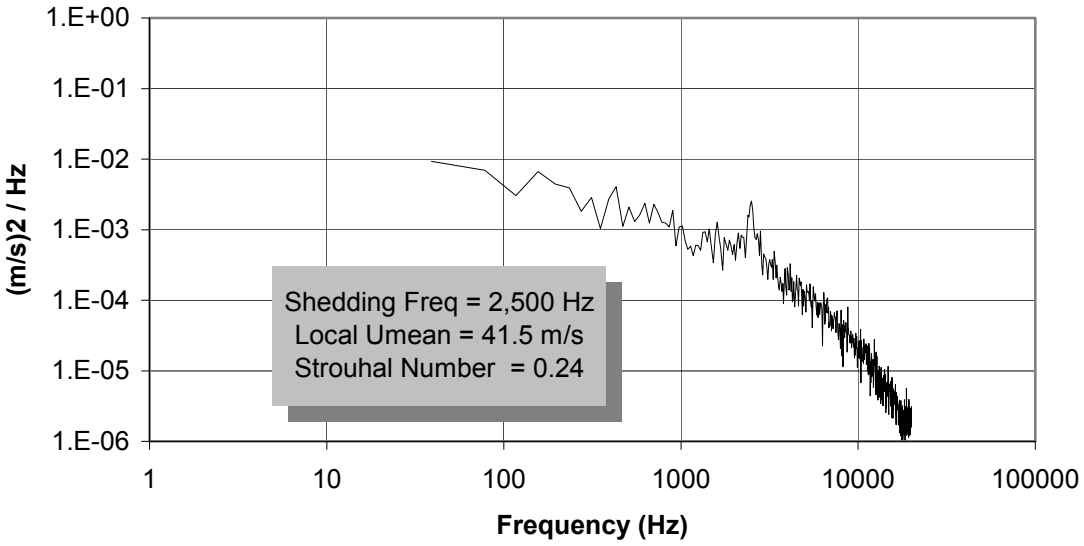

Strouhal Number Survey @ IFA 35 degrees

Ambient Temp = 62F	**Plenum Press = 8.5" H_2O**	**Delta Press = 9" H_2O**
V ref = 60.9 m/s	**Reynolds = 529,285**	**Point number = 28**

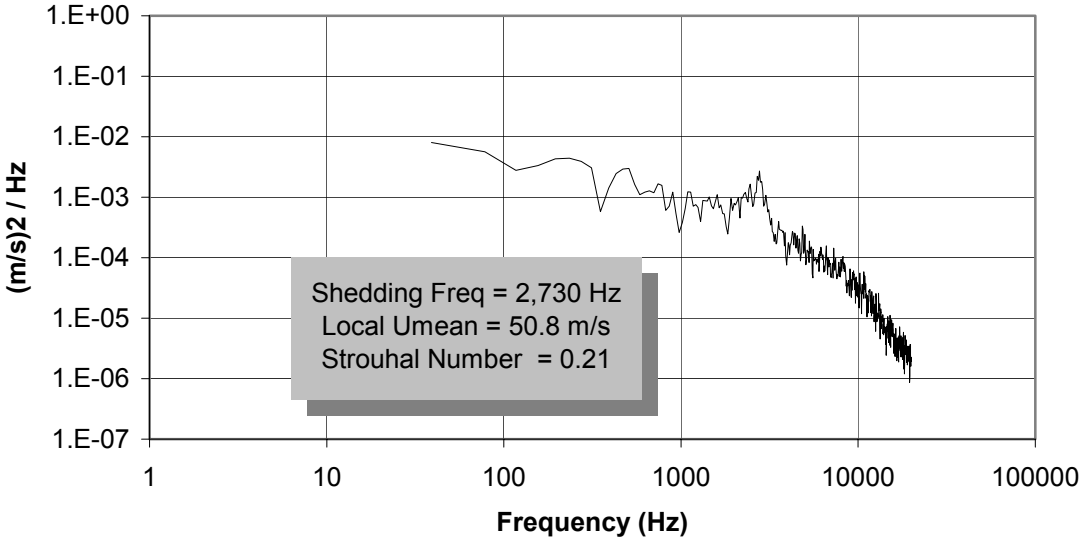

Strouhal Number Survey @ IFA 35 degrees

Ambient Temp = 62F	**Plenum Press = 10.5" H_2O**	**Delta Press = 12.2" H_2O**
V ref = 70.5 m/s	**Reynolds = 612,712**	**Point number = 28**

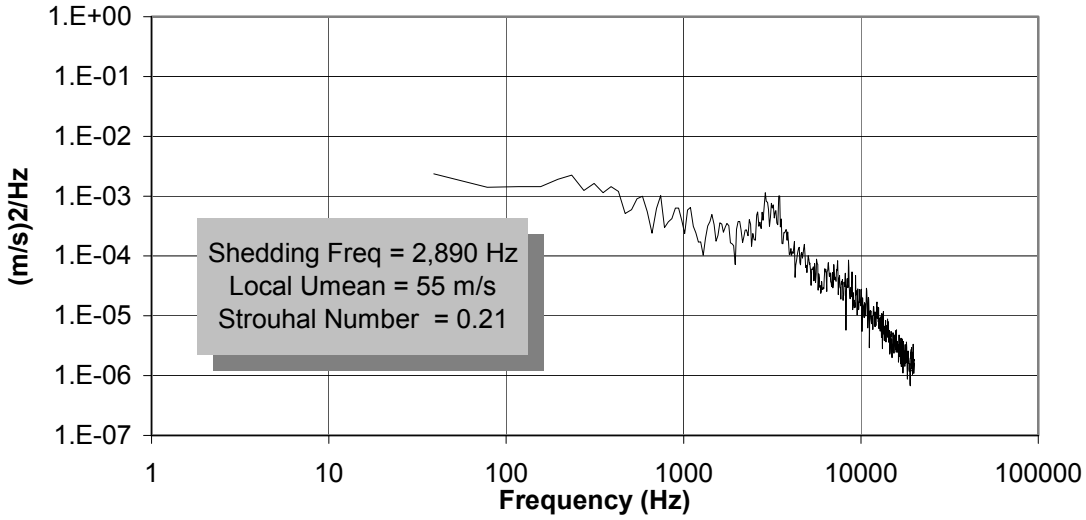

Strouhal Number Survey @ IFA 35 degrees

Ambient Temp = 62F	**Plenum Press = 12" H_2O**	**Delta Press = 13.1" H_2O**
V ref = 72.63 m/s	**Reynolds = 631,444**	**Point number = 28**

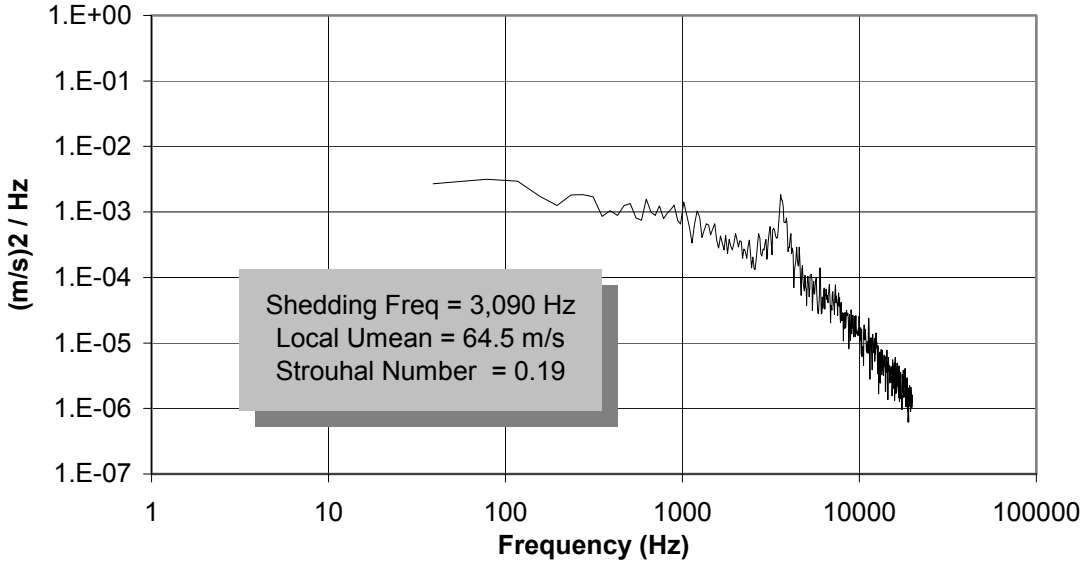

Strouhal Number Survey @ IFA 35 degrees

Ambient Temp = 62F	**Plenum Press = 15.7" H_2O**	**Delta Press = 17" H_2O**
V ref = 82.9 m/s	**Reynolds = 720,611**	**Point number = 28**

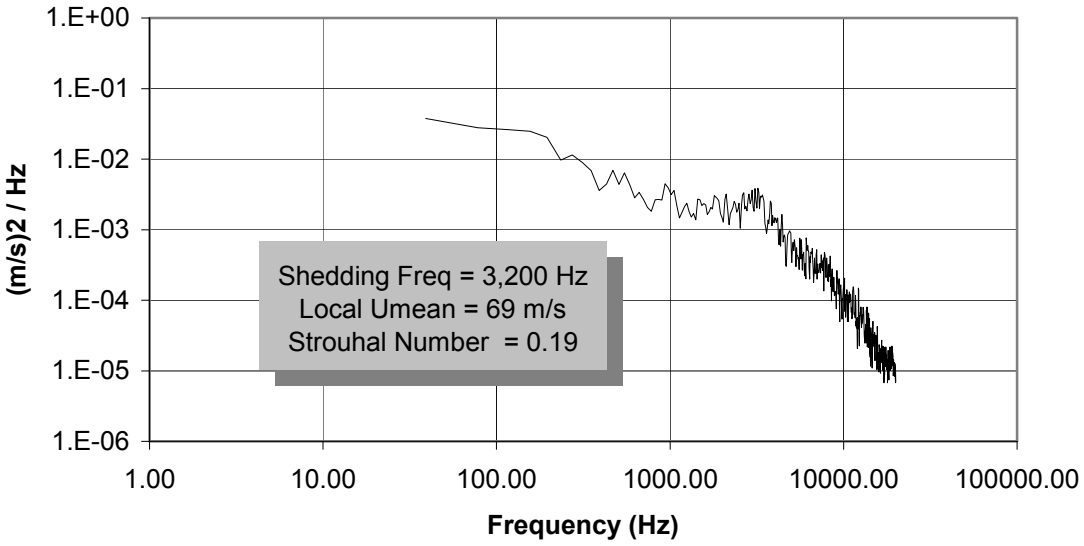

Strouhal Number Survey @ IFA 35 degrees

Ambient Temp = 62F	**Plenum Press = 17"H_2O**	**Delta Press = 18.45" H_2O**
V ref =86.25 m/s	**Reynolds = 749,879**	**Point number = 28**

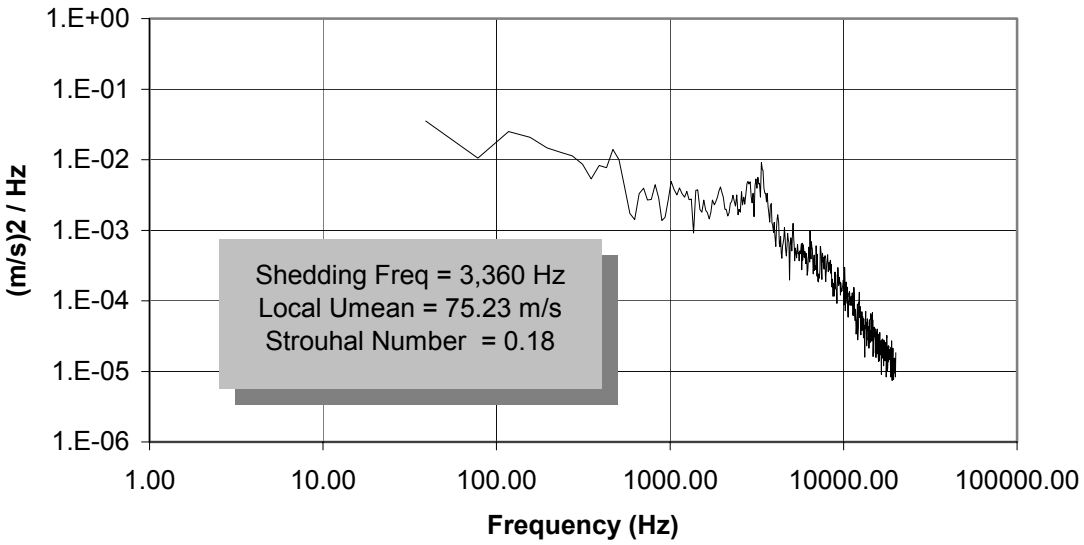

Strouhal Number Survey @ IFA 33 degrees

Ambient Temp = 64F	**Plenum Press = 4.1" H_2O**	**Delta Press = 4.15" H_2O**
V ref = 41.28 m/s	**Reynolds = 358,899**	**Point number = 32**

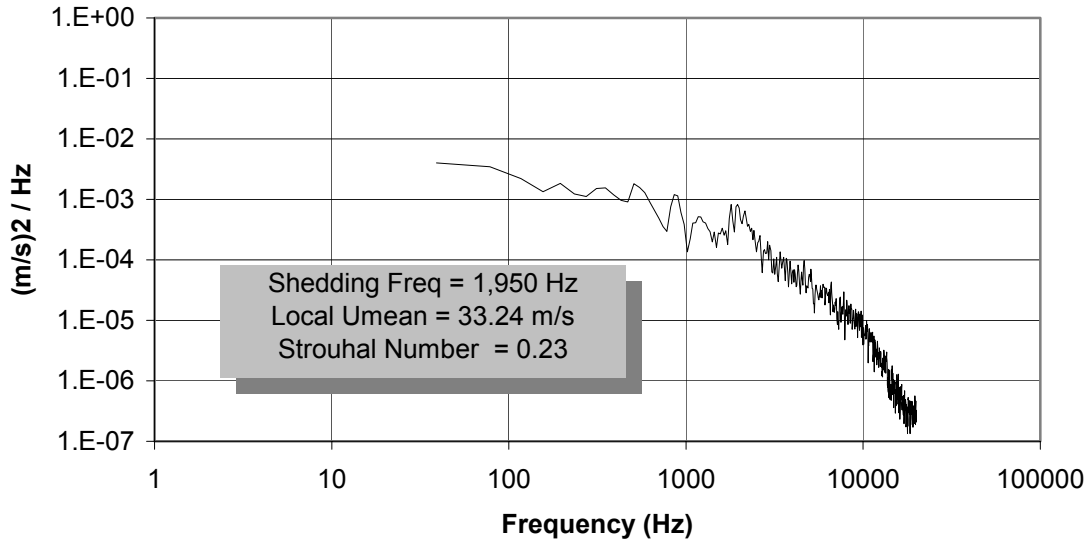

Strouhal Number Survey @ IFA 33 degrees

Ambient Temp = 64F	**Plenum Press = 6.5" H_2O**	**Delta Press = 6.5" H_2O**
V ref = 51.7 m/s	**Reynolds = 449,258**	**Point number = 32**

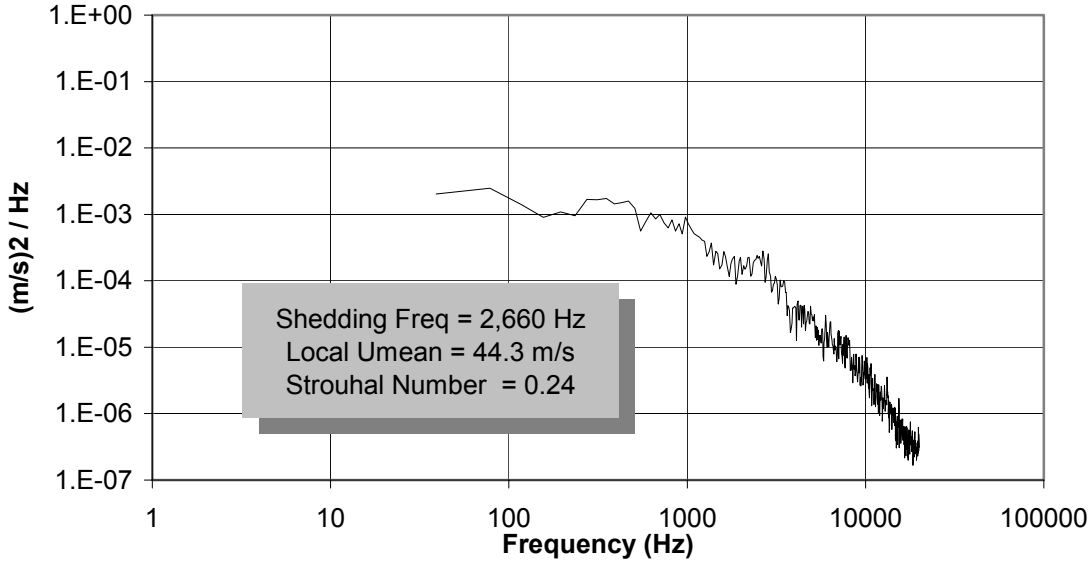

Strouhal Number Survey @ IFA 33 degrees

Ambient Temp = 64F	**Plenum Press = 9.4" H_2O**	**Delta Press = 9.62" H_2O**
V ref = 62.7 m/s	**Reynolds = 545,156**	**Point number = 32**

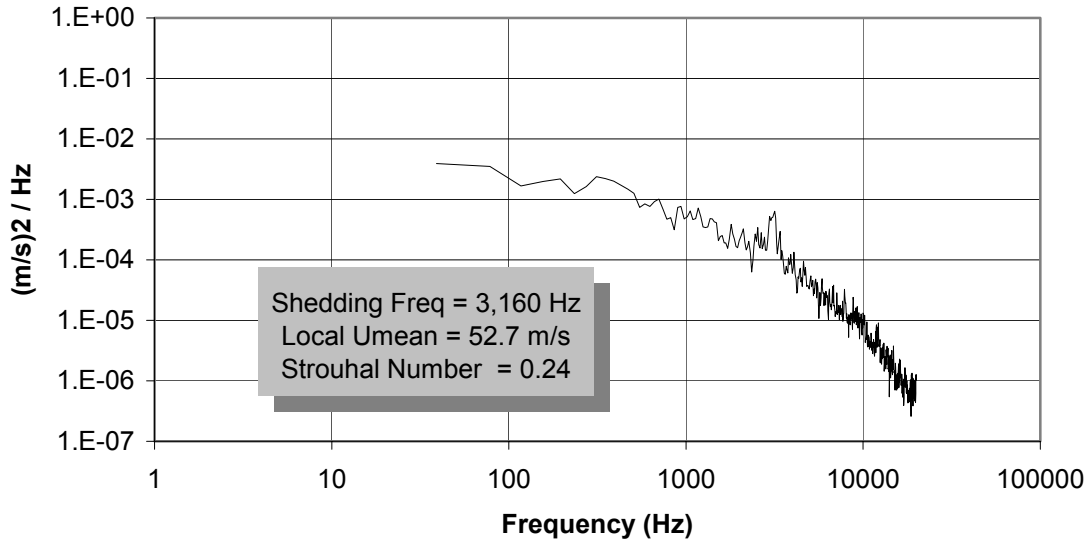

Strouhal Number Survey @ IFA 33 degrees

Ambient Temp = 64F	**Plenum Press = 12.8"H_2O**	**Delta Press = 13" H_2O**
V ref = 72.3 m/s	**Reynolds = 628,470**	**Point number = 32**

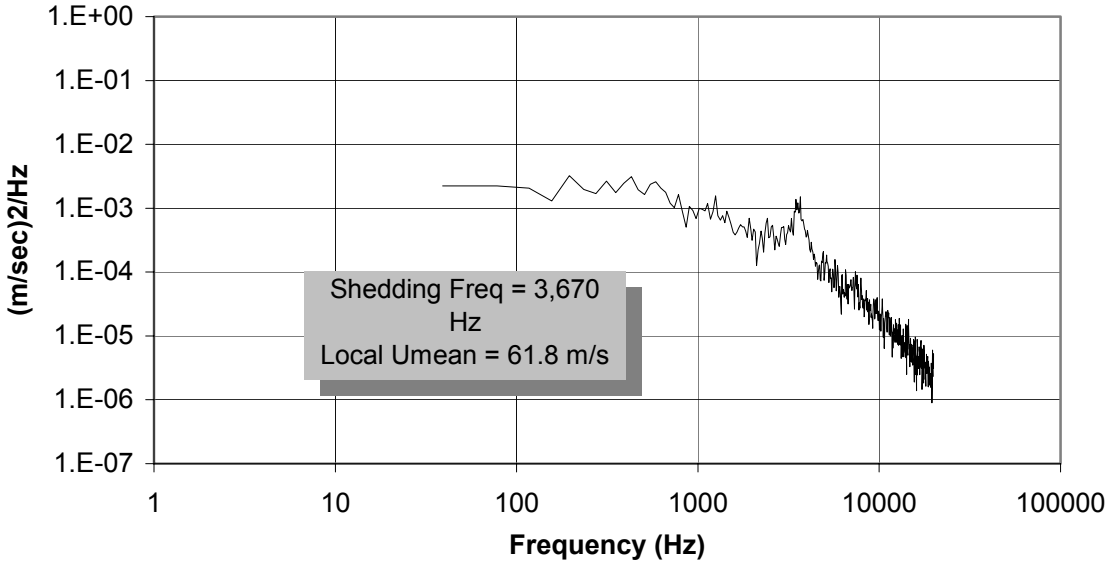

Strouhal Number Survey @ IFA 33 degrees

Ambient Temp = 64F	**Plenum Press = 12.6" H_2O**	**Delta Press = 13" H_2O**
V ref = 72.8 m/s	**Reynolds = 632,655**	**Point number = 32**

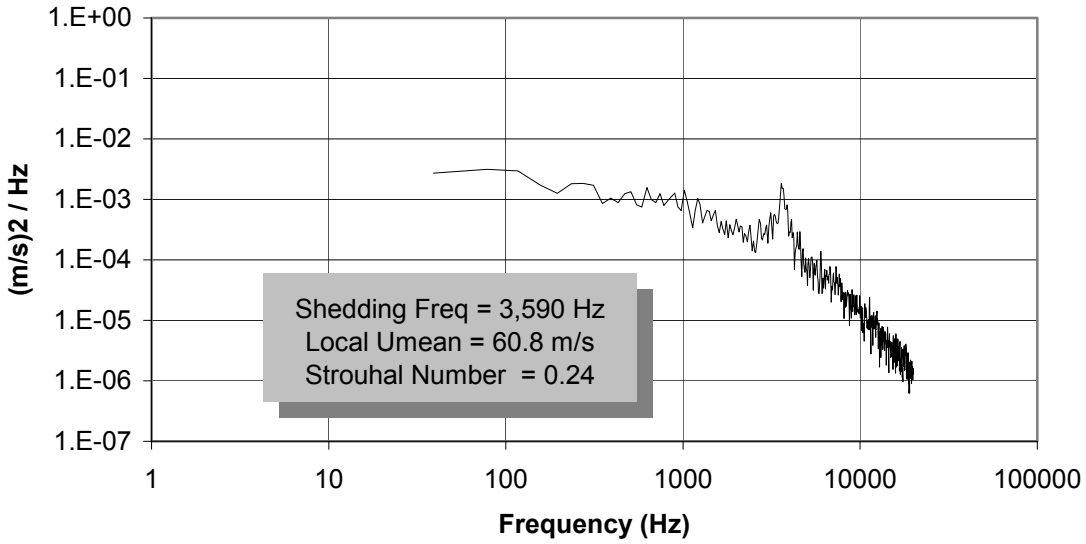

Strouhal Number Survey @ IFA 33 degrees

Ambient Temp = 64F	**Plenum Press = 15.9" H_2O**	**Delta Press = 16.7" H_2O**
V ref = 82.3 m/s	**Reynolds = 715,459**	**Point number = 32**

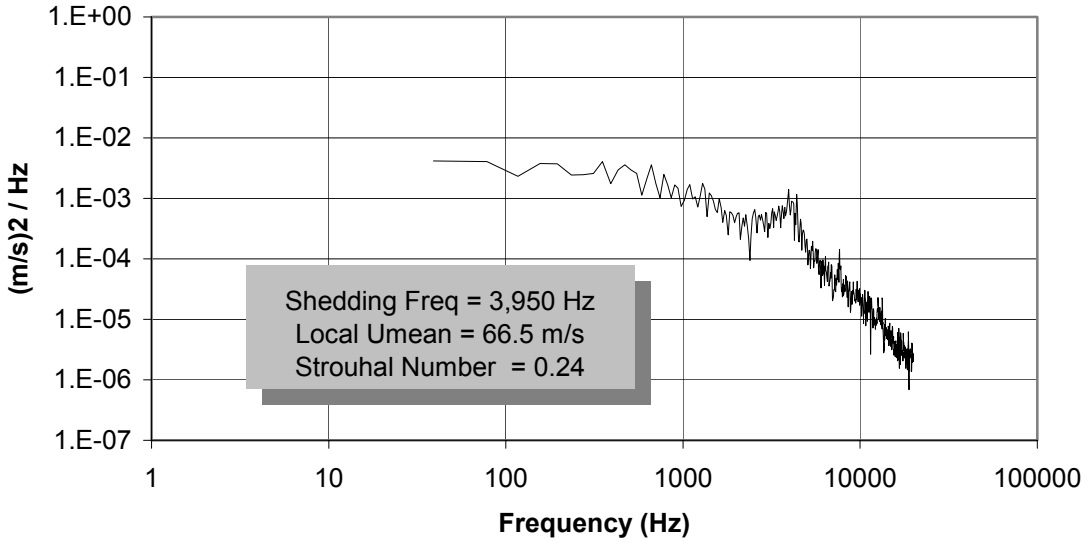

Strouhal Number Survey @ IFA 33 degrees

Ambient Temp = 67F	**Plenum Press = 17.6" H_2O**	**Delta Press = 18.5" H_2O**
V ref = 86.1 m/s	**Reynolds = 748,462**	**Point number = 32**

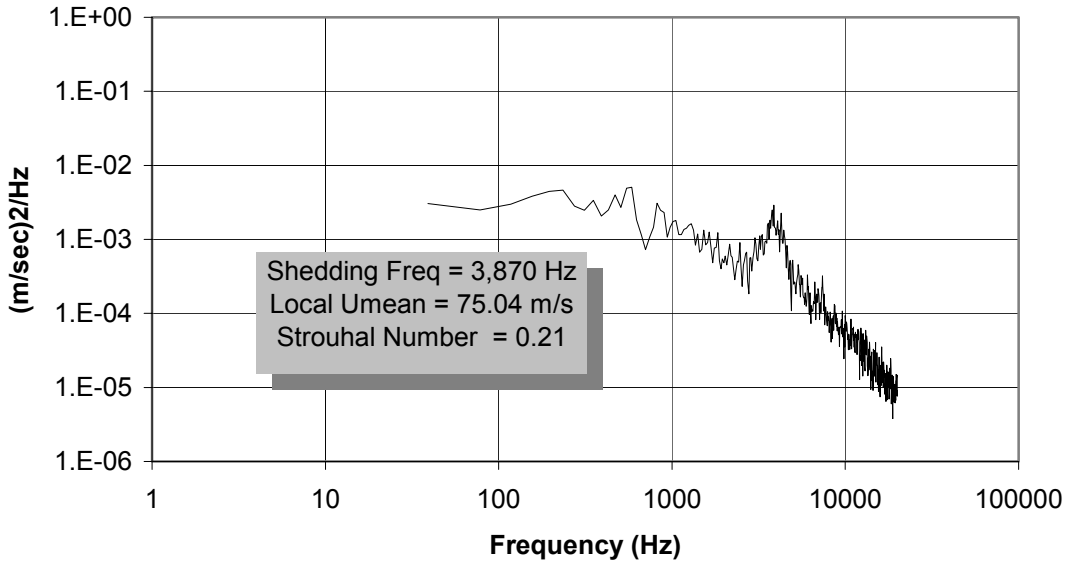

Strouhal Number Survey @ IFA 33 degrees

Ambient Temp = 64F	**Plenum Press = 18.4" H_2O**	**Delta Press = 19.4" H_2O**
V ref = 88.5 m/s	**Reynolds = 769,120**	**Point number = 32**

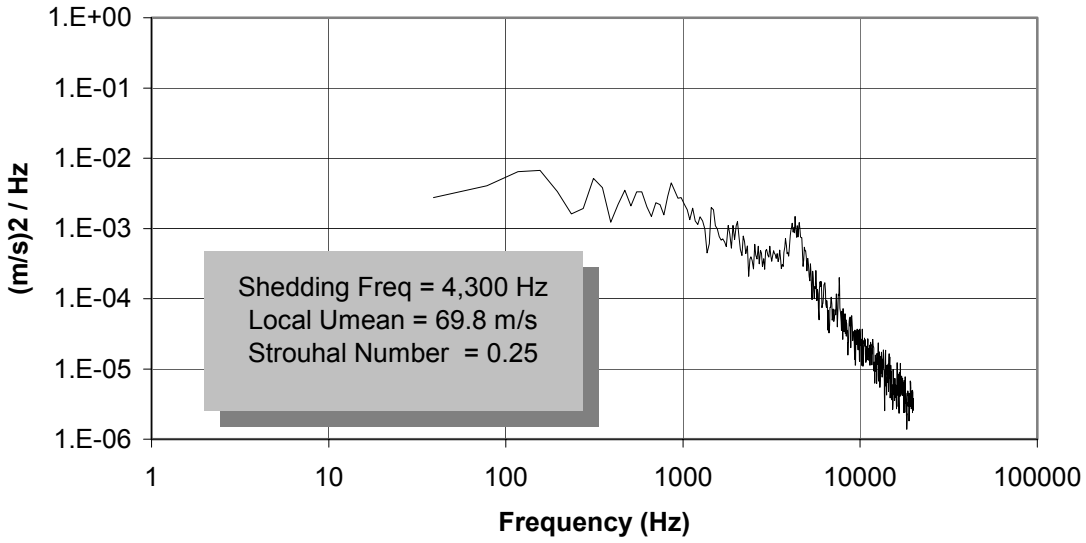

Strouhal Number Survey @ IFA 33 degrees

Ambient Temp = 64F	**Plenum Press = 18.4" H_2O**	**Delta Press = 19.4" H_2O**
V ref = 88.5 m/s	**Reynolds = 791,899**	**Point number = 32**

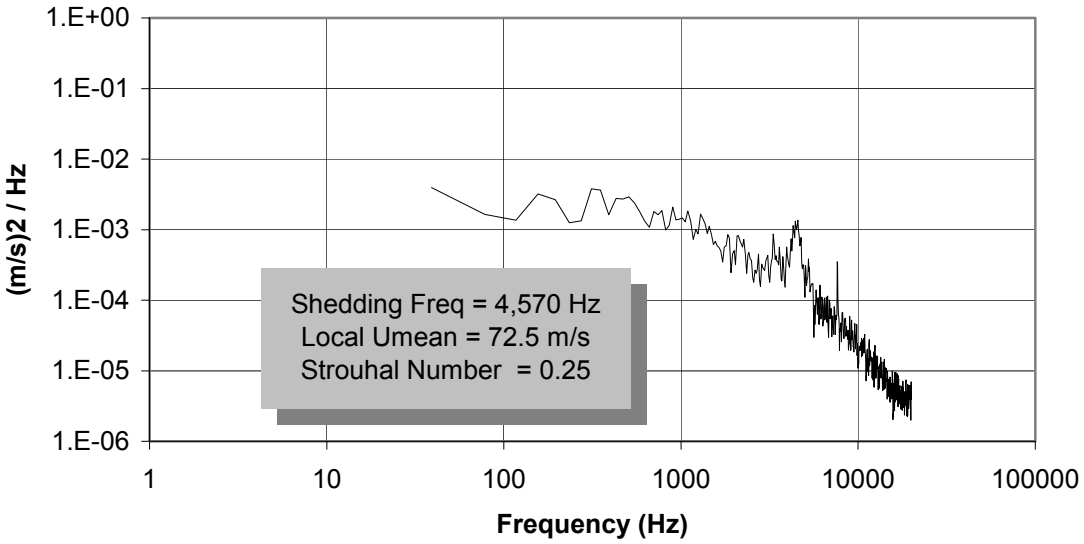

Strouhal Number Survey @ IFA 33 degrees

Ambient Temp = 68F	**Plenum Press = 20.3" H_2O**	**Delta Press = 21.1" H_2O**
V ref = 91.9 m/s	**Reynolds = 798,802**	**Point number = 32**

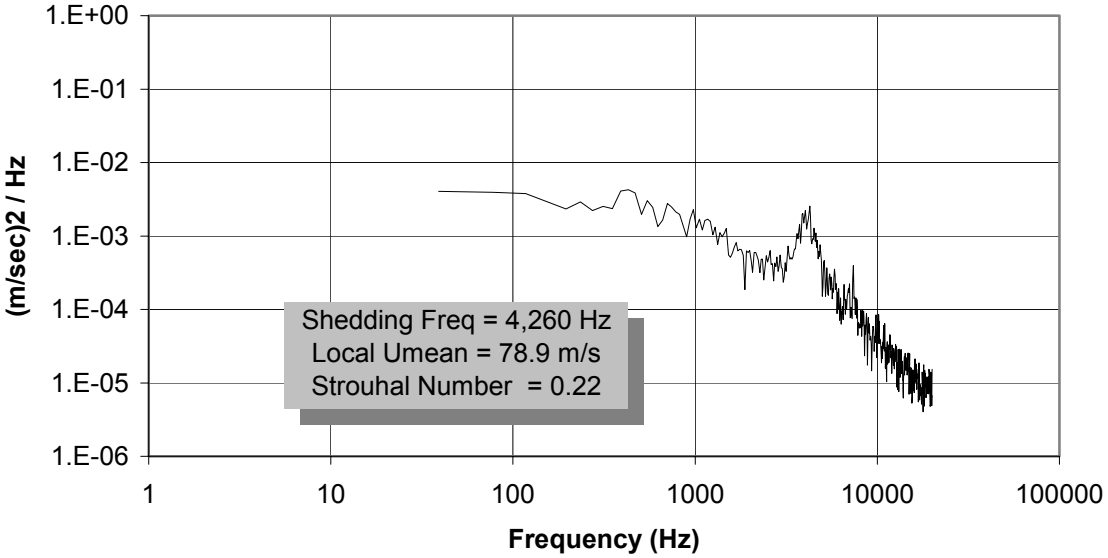

Strouhal Number Survey @ IFA 31 degrees

Ambient Temp = 72F	**Plenum Press = 12.5" H_2O**	**Delta Press = 12.7" H_2O**
V ref = 71.9 m/s	**Reynolds = 625,465**	**Point number = 32**

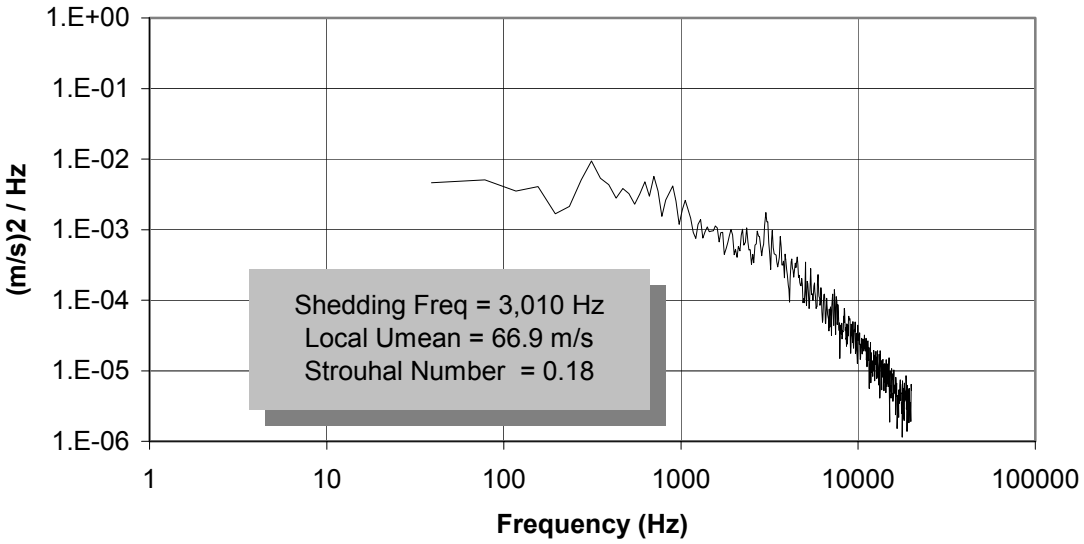

Strouhal Number Survey @ IFA 31 degrees

Ambient Temp = 72F	**Plenum Press = 18.5" H_2O**	**Delta Press = 18.3" H_2O**
V ref = 85.99 m/s	**Reynolds = 747,628**	**Point number = 32**

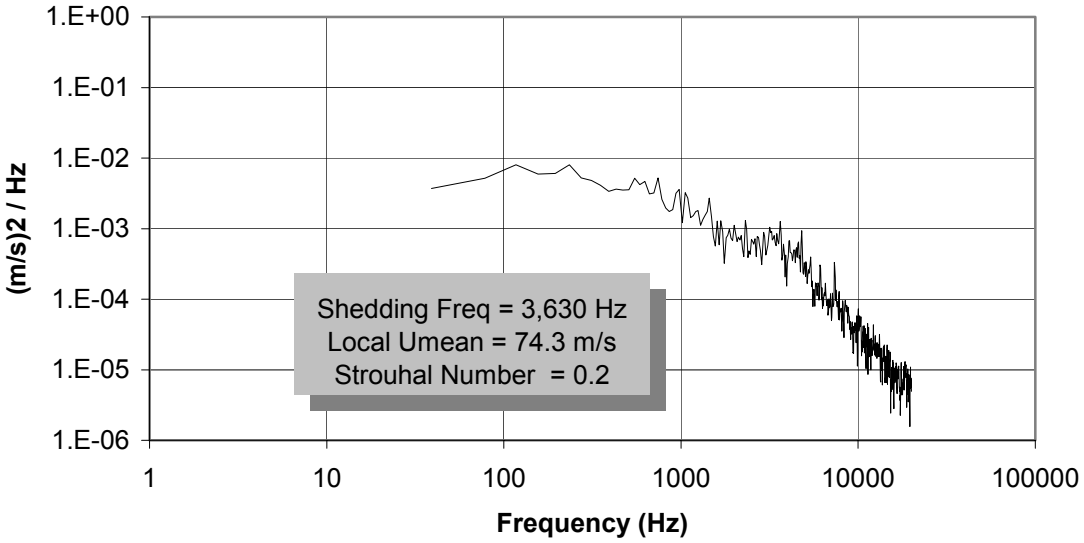

Strouhal Number Survey @ IFA 31 degrees

Ambient Temp = 72F	**Plenum Press = 20.5" H_2O**	**Delta Press = 21.1" H_2O**
V ref = 92.48 m/s	**Reynolds = 804,088**	**Point number = 32**

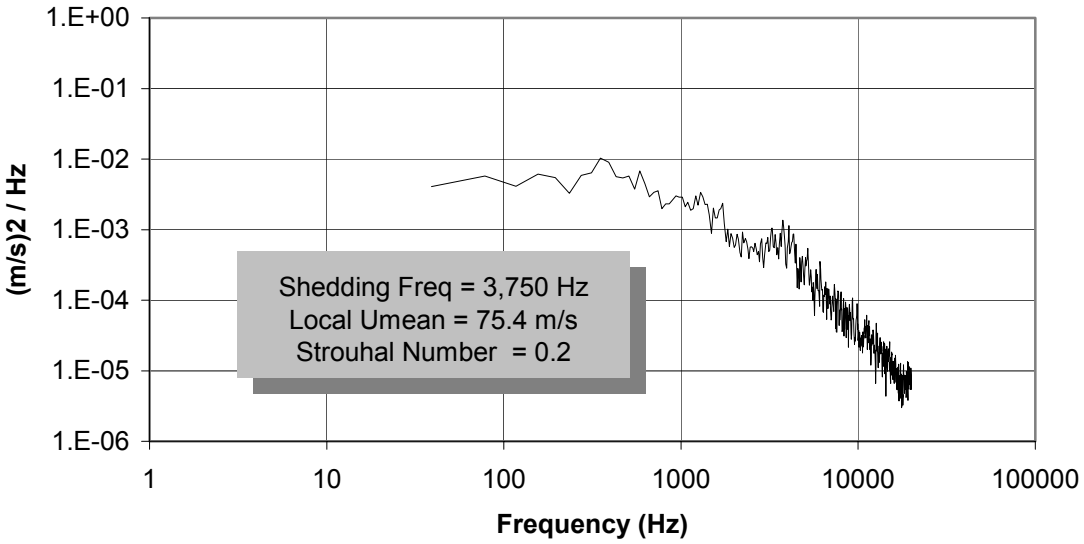

THIS PAGE INTENTIONALLY LEFT BLANK

APPENDIX G: LDV INLET-FLOW SURVEY

Two LDV inlet surveys were performed to check the inlet flow angle and uniform upstream flow. They were performed at inlet-flow angles of 33 and 35 degrees. All surveys were conducted at midspan and at plenum pressure of 304.8 mm (12 inches) of water. Inlet-flow surveys were conducted at Station 1, from the leading edge of blade 3 to the leading edge of blade 4 (span = 152.4 mm), in 6.35 mm increments. The inlet angles versus the non-dimensionalized span between blade 3 and 4 are shown in Figure G.1

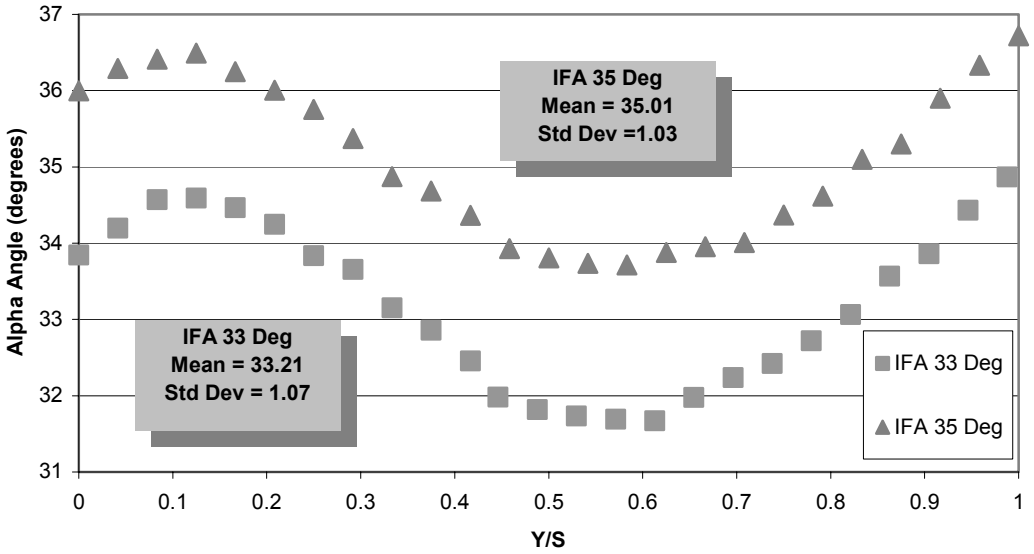

Figure G.1 Inlet-flow angle versus Y/S

From Figure G.1, the mean flow angles of 35.01 and 33.21 were within acceptable bound of 0.3 degrees. The angle variation for 35 degrees and 33 degrees inlet-flow-angle were 3 and 3.2 degrees respectively. The variation in flow angle from blade to blade was as a result of the potential effect of the blades on the approaching flow.

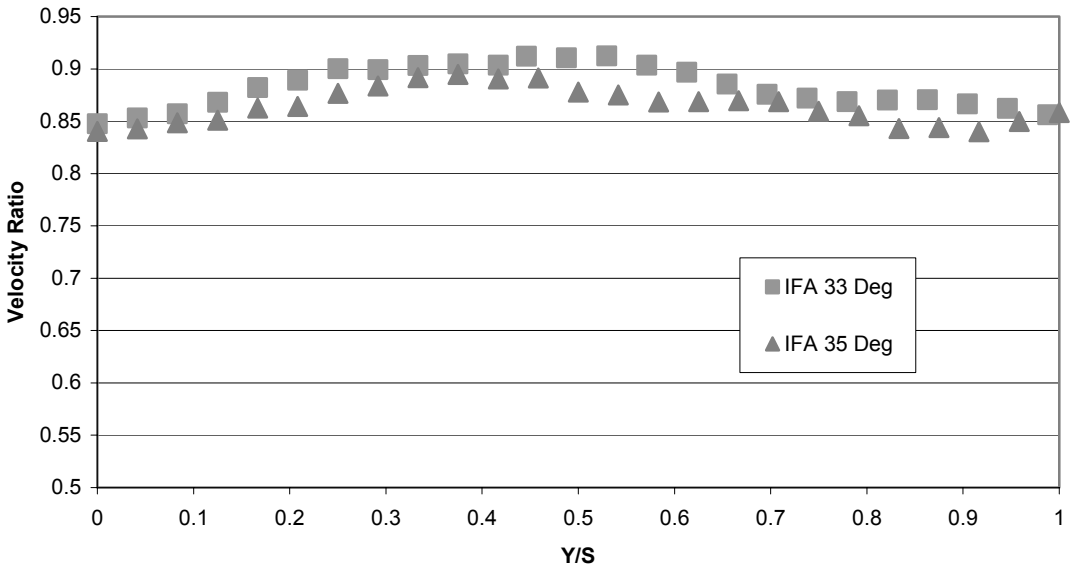

Figure G.2 Inlet-flow velocity ratio versus Y/S

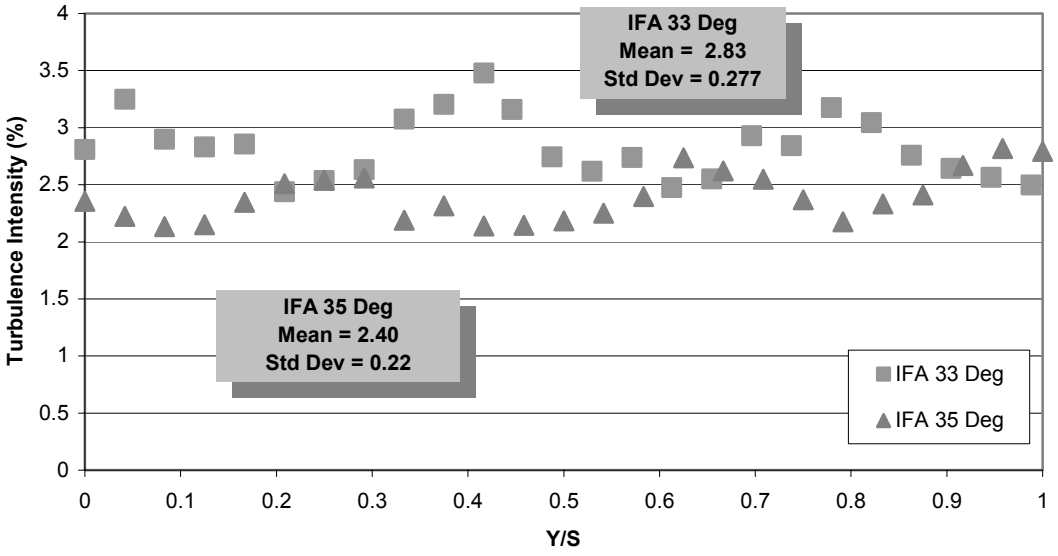

Figure G.3 Inlet-flow turbulence intensity versus Y/S

From Figure G.2, it was observed that the flows at both inlet angles were fairly uniform. The maximum flow variation was 0.054 and 0.065 for 35 degrees and 33 degrees inlet-flow angle respectively. From Figure G.3, it was observed that the average turbulence intensity was 2.4% and 2.83% for inlet-flow angle of 35 degrees and 33 degrees respectively. The turbulence intensity was found to be within the acceptable limits of 3%.

In summary, it was determined from LDV inlet survey that the inlet-flow angles were within acceptable bounds and the inlet flow were uniform with acceptable turbulence intensity of only 3 %.

THIS PAGE INTENTIONALLY LEFT BLANK

APPENDIX H: TABULATED DATA FOR LDV INLET SURVEY

LDV inlet Survey for IFA 35 degrees

Blade spacing = 152.4 mm **Vref = 62.16 m/s** **Re = 540,434**

Y/S	Z(mm)	U / Vref	V / Vref	U Ti (%)	Alpha (Deg)
0.00	-36.60	0.840	0.610	2.355	36.00
0.04	-36.60	0.843	0.619	2.222	36.29
0.08	-36.60	0.848	0.626	2.134	36.41
0.13	-36.60	0.851	0.630	2.151	36.49
0.17	-36.60	0.863	0.632	2.348	36.25
0.21	-36.60	0.864	0.628	2.509	36.01
0.25	-36.60	0.876	0.631	2.540	35.75
0.29	-36.60	0.884	0.627	2.559	35.37
0.33	-36.60	0.892	0.621	2.189	34.87
0.37	-36.60	0.895	0.619	2.316	34.68
0.42	-36.60	0.890	0.609	2.140	34.37
0.46	-36.60	0.891	0.600	2.143	33.93
0.50	-36.60	0.878	0.588	2.184	33.81
0.54	-36.60	0.875	0.584	2.252	33.74
0.58	-36.60	0.868	0.580	2.398	33.71
0.63	-36.60	0.869	0.583	2.737	33.88
0.67	-36.60	0.870	0.586	2.622	33.95
0.71	-36.60	0.869	0.586	2.548	34.01
0.75	-36.60	0.860	0.588	2.368	34.37
0.79	-36.60	0.855	0.590	2.176	34.62
0.83	-36.60	0.843	0.592	2.331	35.10
0.87	-36.60	0.844	0.598	2.410	35.30
0.92	-36.60	0.840	0.608	2.670	35.90
0.96	-36.60	0.850	0.625	2.818	36.33
1.00	-36.60	0.858	0.640	2.793	36.72

LDV inlet Survey for IFA 33 degrees

Blade spacing = 152.4 mm Vref = 63.84 m/s Re = 555,041

Y/S	Z(mm)	U / Vref	V / Vref	U Ti (%)	Alpha (Deg)
0.00	-36.60	0.847	0.568	2.810	33.84
0.04	-36.60	0.853	0.580	3.249	34.20
0.08	-36.60	0.857	0.590	2.897	34.57
0.13	-36.60	0.868	0.599	2.831	34.59
0.17	-36.60	0.882	0.606	2.856	34.47
0.21	-36.60	0.889	0.605	2.439	34.25
0.25	-36.60	0.900	0.603	2.538	33.83
0.29	-36.60	0.899	0.599	2.632	33.65
0.33	-36.60	0.903	0.590	3.076	33.15
0.37	-36.60	0.905	0.584	3.204	32.86
0.42	-36.60	0.904	0.575	3.480	32.46
0.45	-36.60	0.912	0.568	3.159	31.98
0.49	-36.60	0.911	0.573	2.746	31.82
0.53	-36.60	0.912	0.564	2.617	31.74
0.57	-36.60	0.904	0.558	2.740	31.69
0.61	-36.60	0.897	0.553	2.476	31.67
0.65	-36.60	0.886	0.553	2.551	31.98
0.70	-36.60	0.876	0.552	2.929	32.24
0.74	-36.60	0.872	0.554	2.841	32.42
0.78	-36.60	0.869	0.558	3.175	32.72
0.82	-36.60	0.870	0.567	3.045	33.07
0.86	-36.60	0.871	0.578	2.760	33.57
0.90	-36.60	0.866	0.581	2.642	33.86
0.95	-36.60	0.862	0.591	2.564	34.43
0.99	-36.60	0.856	0.597	2.498	34.87

LIST OF REFERENCES

1. Gelder, T.F., Schmidt, J.F., Suder, K.L., and Hathaway, M.D., “Design and Performance of Controlled-Diffusion Stator Compared With Original Double-Circular-Arc Stator”, NASA Technical Paper 2852, March 1989.
2. Sanger, N.L., “The Use of Optimization Techniques to Design Controlled-Diffusion Compressor Blading”, *ASME Journal Of Engineering For Power,* Vol. 105, pp.256-264, 1983.
3. Hansen, D.J., “Investigation of Second Generation Controlled-Diffusion Compressor Blades in Cascade”, Master’s Thesis, Naval Postgraduate School, Monterey, California, September 1995.
4. Schnorenberg, D.G., “Investigation of the Effect of Reynolds Number on Laminar Separation Bubbles on Controlled-Diffusion Compressor Blades in Cascade”, Master’s Thesis, Naval Postgraduate School, Monterey, California, June 1996.
5. Grove, D.V., “Experimental and Numerical Investigation of Second Generation, Controlled-Diffusion, Compressor Blades in Cascade”, Master’s Thesis, Naval Postgraduate School, Monterey, California, June 1997.
6. Nicholls, J.L., "Investigation of Flow Over Second Generation Controlled-Diffusion Blades in a Linear Cascade", Master’s Thesis, Naval Postgraduate School, Monterey, California, September 1999.
7. Carlson, J.R., "Experimental and Computational Investigation of the End Wall Flow in a Cascade of Compressor Blades", Master's Thesis, Naval Postgraduate School, Monterey, California, September 2000.
8. Caruso, T.M., "Three-Component LDV Measurements of Corner Vortices Over Second-Generation, Controlled-Diffusion, Compressor Blades in Cascade", Master's Thesis, Naval Postgraduate School, Monterey, California, September 2001.
9. Brown, P.J., “Experimental Investigation of Votex Shedding in Flow over Second Generation, Controlled Diffusion, Compressor Blades in Cascade”, Master's Thesis, Naval Postgraduate School, Monterey, California, March 2002.
10. Sanger, N.L., and Shreeve, R.P., “Comparison of Calculated and Experimental Cascade Performance for Controlled-Diffusion Compressor Stator Blading”, *ASME Journal of Turbomachinery,* Vol. 108, pp.42-50, July 1986.
11. Grubb, C., Grubbs, L.W., Neuser, M.D., Muller, J., O'Brien, J., "Subsonic Five-Hole Probe Calibration in Non Null-Yaw Mode", AA3802 Term Project, Naval Postgraduate School, Monterey, California, December 1999.
12. Grossman, B.L., "Testing and Analysis of a Transonic Axial Compressor", Master's Thesis, Naval Postgraduate School, Monterey, California, September 1997.

13. Sanz, W and Platzer, M.F., “On the Navier-Strokes Calculation of Separation Bubbles With the New Transition Model”, *ASME Journal of Turbomachinery,* Vol. 120, pp.36-41, Jan 1998.
14. Roshko, A., "On the Development of Turbulent Wakes From Vortex Streets", *NACA Rep.* 1191, 1954.
15. Frank White, “Fluid Mechanics, 4th Edition”, Chapter 5, Dimensional Analysis and Similarity, Figure 5.2, pp. 296, 1999.

INITIAL DISTRIBUTION LIST

1. Defense Technical Information Center
   8725 John J. Kingman Rd., Ste 0944

2. Dudley Knox Library
   Naval Postgraduate School
   Monterey, California

3. Dr. Max F. Platzer
   Department Chairman, Code AA/PL
   Department of Aeronautics and Astronautics
   Naval Postgraduate School

4. Dr. Garth V. Hobson, Code AA/HG
   Department of Aeronautics and Astronautics
   Naval Postgraduate School

5. Dr. Raymond P. Shreeve, Code AA/SF
   Department of Aeronautics and Astronautics
   Naval Postgraduate School

6. Naval Air Warfare Center
   AIR-4.4.7.1 (Attn: Mr. R. Ravindranath)
   Propulsion and Power Engineering, Building 106

7. Naval Air Warfare Center
   AIR-4.4.7.1 (Attn: Mr. M. Klein)
   Propulsion and Power Engineering, Building 106

8. NASA Glenn Research Center
   MS 5-11 (Attn: Dr. C. Hah)
   Cleveland, OH